Computational Mechanics 29 (2002) 340–360 © Springer-Verlag 2002
DOI 10.1007/s00466-002-0347-6

A rate-independent elastoplastic constitutive model for biological fiber-reinforced composites at finite strains: continuum basis, algorithmic formulation and finite element implementation

T. C. Gasser, G. A. Holzapfel

Abstract This paper presents a rate-independent elastoplastic constitutive model for (nearly) incompressible biological fiber-reinforced composite materials. The constitutive framework, based on multisurface plasticity, is suitable for describing the mechanical behavior of biological fiber-reinforced composites in finite elastic and plastic strain domains. A key point of the constitutive model is the use of slip systems, which determine the strongly anisotropic elastic and plastic behavior of biological fiber-reinforced composites. The multiplicative decomposition of the deformation gradient into elastic and plastic parts allows the introduction of an anisotropic Helmholtz free-energy function for determining the anisotropic response. We use the unconditionally stable backward-Euler method to integrate the flow rule and employ the commonly used elastic predictor/plastic corrector concept to update the plastic variables. This choice is expressed as an Eulerian vector update the Newton's type, which leads to a numerically stable and efficient material model. By means of a representative numerical simulations the performance of the proposed constitutive framework is investigated in detail.

Keywords Biomechanics, Soft Tissue, Elastoplasticity, Anisotropy, Finite Element Method

1 Introduction

The evaluation of the overall properties of fiber-reinforced composites are of increasing industrial and scientific interest. The proposed constitutive framework, with the associated algorithmic formulation and the finite element implementation has wide engineering and scientific applications such as the mechanical analysis of textiles, elastoplastic modeling of pneumatic membranes [43] and the modeling of municipal solid waste landfills [13]. In addition, carbon-black or silicate filled rubber shows, beside the viscoelastic effects, typical amplitude-dependent plastic changes of the microstructure [24]. It is assumed that the polymer molecules (chains) slip relative to the filler surface, which is more general mechanism than that considered within this work.

The application of the proposed constitutive framework is addressed to biomechanics. For some aspects soft biological tissues can be treated as highly deformable fiber-reinforced composite structures such as an artery [21]. It is known, that, from an engineering point of view, soft biological tissues undergo plastic strains when they are loaded far beyond the physiological domain. The structural mechanisms during this type of deformation, however, remains still unclear.

Already in 1967, Ridge and Wright [44] reported that the extension behavior of skin showed typical yielding and failure regions, and Abrahams [1] pointed out that preconditioning of a tendon leads to an *irreversible* increase of its length. Experimental investigations performed by Salunke and Topoleski [45] showed that the overall mechanical response of plaque with a low amount of calcium leads to 'non-recoverable' deformation if subjected to phasic cyclic compressive loading. Sverdlik and Lanir [55] recommended to include a 'plastic pre-conditioning' contribution (in terms of viscoplasticity and rate-independent plasticity) to the constitutive formulation for tendons in order to get a better agreement with experimental data. For vascular tissue Oktay et al. [40] reported a (remaining) mean increase of 13% at zero pressure of (healthy) common carotid arteries following balloon angioplasty. Therein it was documented that the plastic deformation is coupled with damage-based softening of the arterial response.

In addition, however, several works document that failure of soft biological tissue is not accompanied with non-recoverable deformations. For example, Emery et al. [14] observed damage based softening of the left ventricular myocardium of a rate by no changes in the unloaded segment length after overstretching the material.

A hypothetical explanation of these two contrary mechanical behaviors of soft biological tissues under failure (i.e. *yielding* and *softening*) was given by Parry et al. [42]. These authors reported that there are two competing factors which may determine the collagen fibril diameter (type I) of a connective tissue: (i) if collagen fibrils have to carry high tensile stress they need to be large in diameter in order to maximize the density of intrafibrillar covalent crosslinks, and (ii): in order to capture non-recoverable creep after removal of the load, the tissue needs sufficient interfibrillar non-covalent crosslinks. This can be achieved by numerous collagen fibrils small in diameter such that the surface area per unit mass increases.

Received: 12 December 2001 / Accepted: 14 June 2002

T. C. Gasser, G. A. Holzapfel (✉)
Institute for Structural Analysis – Computational Biomechanics
Graz University of Technology, 8010 Graz,
Schiesstattgasse 14-B, Austria
e-mail: gh@biomech.tu-graz.ac.at

Financial support for this research was provided by the Austrian Science Foundation under START-Award Y74-TEC. This support is gratefully acknowledged.

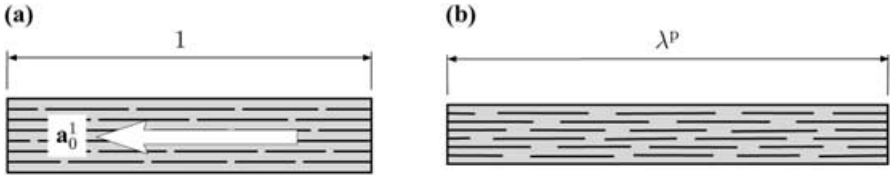

Fig. 1. Fiber-reinforced composite with one family of fibers, characterized by the unit direction vector $\mathbf{a}_0^1$: (**a**) before plastic deformation (length 1), and (**b**) after plastic deformation (plastic stretch λ^p). Plastic deformation is accumulated by relative slips of the fibers

Based on these findings one can postulate (i) that damage in connective tissue incorporating *thick* collagen fibrils, is mainly governed by a relative sliding mechanism of collagen fibrils, and non-recoverable creep evolves. Hence, it is suggested that the matrix material is responsible for the plastic deformation. In this case the mechanical response may be described by the theory of plasticity, which is one goal of the present work. There against, (ii) damage evolves in connective tissue incorporating thin collagen fibrils due to breakage of collagen and collagen cross-links. This failure pattern is clearly addressed to damage mechanics (as introduced by, for example, Kachanov [22]), which causes softening (weakening) of the material response. This is in agreement with the fact, that no plastic mechanisms can be explained on a molecular level of collagen fibrils. A similar (hypothetical) explanation of these two contrary failure mechanisms of soft biological tissues may be found in a recent paper by Ker et al. [25], which is concerned with mammalian tendons. In practice, both of the above described mechanisms will be present in soft biological tissues. This can be observed, in general, in form of various *in vitro* experiments where softening and non-recoverable deformations are coupled, see, for example, Oktay et al. [40].

From the modeling point of view, there are several elastoplastic constitutive formulations available in the literature that include finite element implementations of fiber-reinforced composites, see, for example, [43]. In addition, Ogden and Roxburgh [39] use a modified pseudo-elasticity theory in order to model the response of filled rubber including residual strains after unloading. However, there are only a few constitutive descriptions known in the literature which include plastic phenomena of biological tissues. For example, the works by Tanaka and Yamada [56] and Tanaka et al. [57] deal with (plastic) dissipative behavior of arteries within the physiological range of loading by means of a viscoplastic formulation. In contrast to that, several constitutive formulations can be found in the literature dealing with damage-based softening of soft biological tissues, see, for example, the work by Emery et al. [14] for the left ventricular myocardium, Liao and Belkoff [27] for ligaments or Hokanson and Yazdani [18] for arteries.

Although the structural mechanisms responsible for the plastic deformation as postulated by Parry et al. [42] is not experimentally identified, we follow this concept and describe plastic effects on the basis of this approach, which differs significantly from the approaches by Reese [43] or Tanaka et al. [57]. We use a structural-based formulation and focus attention on the description of rate-independent inelastic deformations of fiber-reinforced composites exposed to loadings beyond the yielding limit. Such high load ranges arise, for example, in biomechanics, during Percutaneous Transluminal Angioplasty (PTA), which is a clinical treatment used world wide to enlarge the lumen of an atherosclerotic artery [7]. It is assumed that due to this loadings, fibers of the composite slip relative to each other so that plastic deformations in the matrix evolve, as it is postulated for tendons by Parry et al. [42]. Figure 1 attempts to show this mechanism, whereby (a) illustrates the composite before and (b) after plastic deformation.

In this present work we focus on the elastoplastic modeling of fiber-reinforced composites in the finite strain domain and do not include damage-based softening of the material. The formulation is based on a macroscopic (effective) continuum approach, in which a material point reflects the overall response of a statistically homogeneous representative volume element (RVE), as defined in Krajcinovic [26]. Furthermore, we apply homogeneous strain distributions over the RVE, meaning that perfect bonds between fibers and matrix are assumed, and homogeneous boundary conditions on the RVE are applied.

The concept of rate-independent multisurface plasticity is employed. Multisurface plasticity models have been well-known in engineering mechanics for several decades. The most classical approach is the so-called *Tresca* model [17]; however, may other efficient constitutive models are known, for example, in the context of geomechanics [11, 12], metal plasticity [47] or crystal plasticity [2].

In view of the organized structure of fiber-reinforced composites it is assumed that the plastic deformation is kinematically constraint. The presented approach is similar to that used for the description of crystal plasticity [2], where the plastic strains are solely due to the plastic slip on given slip planes [23, 32], and references therein. We borrow this terminology from crystal plasticity and define the slip systems by a set $\{\mathbf{a}_0^\alpha; \alpha = 1, \ldots, n\}$ of n unit vectors, reflecting the structural architecture of the composite. Based on the idea of the theory of fiber-reinforced composites we use these structural measures to introduce an anisotropic free-energy function (for the description of the elastic part of the deformation see [19, 20, 54]. In order to determine the plastic deformation we introduce a flow rule, which is motivated by the architecture of the composite.

The continuum mechanical framework is set up by the introduction of a convex, but non-smooth, yield surface in the (*Mandel*) stress space. The irreversible nature of the plastic deformation is enforced by the

Karush-Kuhn-Tucker loading/unloading conditions. This description is standard in computational plasticity [48, 50] and has been used successfully in the past. For the finite element implementation of the constitutive model we employ the classical elastic predictor/plastic corrector method, which is based on a backward-Euler discretization of the evolution equation [32, 48, 50]. This approach is originally proposed by Wilkins [60] and Moreau [35, 36], and it leads to a robust and efficient update of the plastic variables. Finally, the algorithmic stress tensor and the algorithmic tangent moduli are derived explicitly so that the global equilibrium can be solved within the finite element method by using the incremental/iterative solution techniques of Newton's type [9, 61].

2
Multiplicative multisurface plasticity

In this chapter we present briefly the continuum mechanical theory of multiplicative multisurface plasticity suitable for describing the strongly anisotropic mechanical behavior of fiber-reinforced composites. The theory is based on a multiplicative split of the deformation gradient into elastic and plastic parts, for which purpose we introduce a local macro-stress-free intermediate configuration. This framework is well-known in computational plasticity [50] and suitable for describing the finite strains which are observed experimentally in tests on, for example, biological soft tissues.

Finally, the constitutive model, which is based on the theory of fiber-reinforced composites, is presented. It is characterized by an anisotropic Helmholtz free-energy function and replicates the basic mechanical features of arterial walls in a realistic and accurate manner.

2.1
Basic notation

Let Ω_0 be the (fixed) reference configuration of the continuous body of interest (assumed to be stress-free) at reference time $t_0 = 0$. We use the notation $\boldsymbol{\chi}(\bullet, t) : \Omega_0 \rightarrow \mathbb{R}^3$ for the motion of the body which transforms a typical point $\mathbf{X} \in \Omega_0$ to a position $\mathbf{x} = \boldsymbol{\chi}(\mathbf{X}, t) \in \Omega$ in the deformed configuration, denoted Ω, where $t \in [0, T]$ is in the closed time interval of interest. Further, let $\mathbf{F}(\mathbf{X}, t) = \partial\boldsymbol{\chi}(\mathbf{X}, t)/\partial\mathbf{X}$ be the deformation gradient and $J(\mathbf{X}, t) = \det \mathbf{F} > 0$ the volume ratio.

In the neighborhood of every $\mathbf{X} \in \Omega_0$ we consider the local multiplicative decomposition

$$\mathbf{F} = \mathbf{F}^{\mathrm{e}}\mathbf{F}^{\mathrm{p}} \ , \tag{1}$$

where $\mathbf{F}^{\mathrm{p}}(\mathbf{X}, t)$ maps a referential point $\mathbf{X} \in \Omega_0$ into $\tilde{\mathbf{X}}$ (located at a macro-stress-free (plastic) intermediate configuration) and $\mathbf{F}^{\mathrm{e}}(\tilde{\mathbf{X}}, t)$ maps this point $\tilde{\mathbf{X}}$ into its spatial position $\mathbf{x} \in \Omega$, as depicted in Fig. 2.

In addition, following [15, 37], we consider the multiplicative decompositions of $\mathbf{F}^{\mathrm{e}}$ and $\mathbf{F}^{\mathrm{p}}$ into spherical and unimodular parts, i.e.

$$\begin{aligned} \mathbf{F}^{\mathrm{e}} &= J^{\mathrm{e}1/3}\bar{\mathbf{F}}^{\mathrm{e}}, \quad J^{\mathrm{e}} = \det \mathbf{F}^{\mathrm{e}} > 0, \\ \mathbf{F}^{\mathrm{p}} &= J^{\mathrm{p}1/3}\bar{\mathbf{F}}^{\mathrm{p}}, \quad J^{\mathrm{p}} = \det \mathbf{F}^{\mathrm{p}} > 0 \ . \end{aligned} \tag{2}$$

With Eqs. (2) and the assumption $J^{\mathrm{p}} = 1$, the usual assumption in metal plasticity [28], Eq. (1) reads

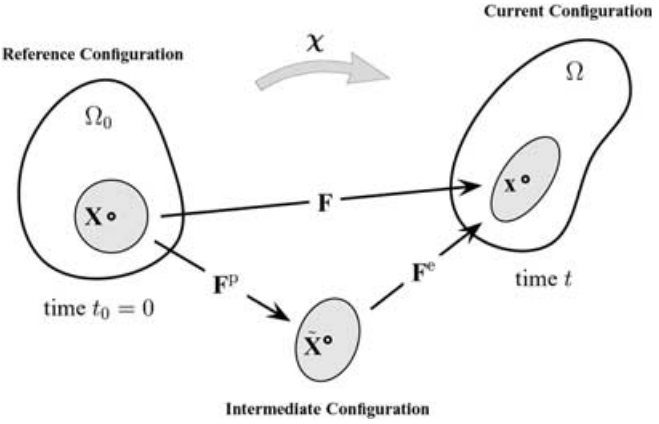

Fig. 2. Local multiplicative decomposition $\mathbf{F} = \mathbf{F}^{\mathrm{e}}\mathbf{F}^{\mathrm{p}}$ of the deformation gradient

$$\mathbf{F} = J^{1/3}\bar{\mathbf{F}}^{\mathrm{e}}\mathbf{F}^{\mathrm{p}}, \quad J = J^{\mathrm{e}} = \det \mathbf{F}^{\mathrm{e}} > 0 \ . \tag{3}$$

We now introduce the elastic right and left Cauchy-Green measures in the usual way,

$$\mathbf{C}^{\mathrm{e}}(\mathbf{X}, t) = \mathbf{F}^{\mathrm{e}\mathrm{T}}\mathbf{F}^{\mathrm{e}} = J^{2/3}\bar{\mathbf{C}}^{\mathrm{e}}, \quad \bar{\mathbf{C}}^{\mathrm{e}} = \bar{\mathbf{F}}^{\mathrm{e}\mathrm{T}}\bar{\mathbf{F}}^{\mathrm{e}} \ , \tag{4}$$

$$\mathbf{b}^{\mathrm{e}}(\mathbf{x}, t) = \mathbf{F}^{\mathrm{e}}\mathbf{F}^{\mathrm{e}\mathrm{T}} = J^{2/3}\bar{\mathbf{b}}^{\mathrm{e}}, \quad \bar{\mathbf{b}}^{\mathrm{e}} = \bar{\mathbf{F}}^{\mathrm{e}}\bar{\mathbf{F}}^{\mathrm{e}\mathrm{T}} \ . \tag{5}$$

The symmetric and positive definite strain tensors $\bar{\mathbf{C}}^{\mathrm{e}}$ and $\bar{\mathbf{b}}^{\mathrm{e}}$ introduced through Eqs. $(4)_2$ and $(5)_2$ are the modified right and left Cauchy-Green tensors, respectively.

In order to describe the kinematics of plastic deformations we follow [30] and introduce a consistent transformation of the spatial velocity gradient $\mathbf{l} = \dot{\mathbf{F}}\mathbf{F}^{-1}$ to the intermediate configuration, i.e.

$$\mathbf{L} = \mathbf{F}^{\mathrm{e}-1}\mathbf{l}\mathbf{F}^{\mathrm{e}} = \mathbf{L}^{\mathrm{e}} + \mathbf{L}^{\mathrm{p}} \ , \tag{6}$$

$$\mathbf{L}^{\mathrm{e}} = \mathbf{F}^{\mathrm{e}-1}\dot{\mathbf{F}}^{\mathrm{e}}, \quad \mathbf{L}^{\mathrm{p}} = \dot{\mathbf{F}}^{\mathrm{p}}\mathbf{F}^{\mathrm{p}-1} \ , \tag{7}$$

where the superposed dot denotes the material time derivative. The stress measure work-conjugate to $\mathbf{L}$ turns out to be the (non-symmetric) Mandel stress tensor, denoted by Σ. Consequently, the stress power $\mathscr{P}$ per unit reference volume is given as

$$\mathscr{P} = \Sigma : \mathbf{L}, \quad \Sigma = \mathbf{F}^{\mathrm{e}\mathrm{T}}(\mathbf{g}\boldsymbol{\tau})\mathbf{F}^{\mathrm{e}-\mathrm{T}} \ , \tag{8}$$

where $\mathbf{g}$ and $\boldsymbol{\tau}$ denote the Eulerian metric and the symmetric (spatial) Kirchhoff stress tensor, respectively.

2.2
Anisotropic elastic stress response

In order to describe the anisotropic elastic stress response of fiber-reinforced composites, we assume the existence of a Helmholtz free-energy function Ψ and use it in the *decoupled* form

$$\begin{aligned} \Psi(\mathbf{F}^{\mathrm{e}}, \mathbf{a}_0^1, \mathbf{a}_0^2, \ldots, \mathbf{a}_0^n, A) &= \Psi_{\mathrm{macro}}(\mathbf{F}^{\mathrm{e}}, \mathbf{a}_0^1, \mathbf{a}_0^2, \ldots, \mathbf{a}_0^n) \\ &\quad + \Psi_{\mathrm{micro}}(A) \ . \end{aligned} \tag{9}$$

Here the free-energy function Ψ_{macro} describes the *macroscopic* stress response and Ψ_{micro} the energy stored in the *microstructure* due to hardening effects. The anisotropy of the composite is assumed to be caused by

the fiber reinforcement, which is characterized by the set $\{\mathbf{a}_0^\alpha; \alpha = 1, \ldots, n\}$ of unit vectors.

Furthermore, we assume that the energy stored in the microstructure depends on a single scalar A, which plays the role of a hardening variable. It is an internal variable and is referred to as the equivalent plastic strain in the constitutive theory of plasticity.

The plastic dissipation $\mathscr{D}^{\mathrm{p}}$ per unit reference volume of the considered isothermal process (we assume a purely mechanical theory) is given by the Clausius-Planck inequality [19]

$$\mathscr{D}^{\mathrm{p}} = \boldsymbol{\Sigma} : \mathbf{L} - \dot{\Psi} \geq 0 \ . \tag{10}$$

Using Eqs. (9) and $(7)_1$, the material time derivative of Ψ leads to

$$\dot{\Psi} = \mathbf{F}^{\mathrm{eT}} \frac{\partial \Psi}{\partial \mathbf{F}^{\mathrm{e}}} : \mathbf{L}^{\mathrm{e}} + \frac{\partial \Psi}{\partial A} \dot{A} \ . \tag{11}$$

With this result and Eq. (6) the Clausius-Planck inequality (10) reads

$$\mathscr{D}^{\mathrm{p}} = \left(\boldsymbol{\Sigma} - \mathbf{F}^{\mathrm{eT}} \frac{\partial \Psi}{\partial \mathbf{F}^{\mathrm{e}}} \right) : \mathbf{L}^{\mathrm{e}} + \boldsymbol{\Sigma} : \mathbf{L}^{\mathrm{p}} - \frac{\partial \Psi}{\partial A} \dot{A} \geq 0 \ . \tag{12}$$

Before proceeding to examine the constitutive relation for the Mandel stress tensor $\boldsymbol{\Sigma}$ (the macro-stress) and the plastic dissipation $\mathscr{D}^{\mathrm{p}}$ we introduce the micro-stress $B = \partial \Psi_{\mathrm{micro}} / \partial A$, work conjugate to the hardening variable A [32]. Using standard arguments we find from Eq. (12) that

$$\boldsymbol{\Sigma} = \mathbf{F}^{\mathrm{eT}} \frac{\partial \Psi}{\partial \mathbf{F}^{\mathrm{e}}}, \quad \mathscr{D}^{\mathrm{p}} = \boldsymbol{\Sigma} : \mathbf{L}^{\mathrm{p}} - B\dot{A} \geq 0 \ . \tag{13}$$

In order to compute the stress response and the plastic dissipation of the material model via Eq. (13) the plastic part of the deformation must be determined. The necessary continuum mechanical basis is developed in the next section.

2.3 Yield criterion functions and evolution equations for multisurface plastic flow

For providing equations suitable to determine the plastic part of the deformation we follow the classical approach described in [50] (for the used notation see reference [48]). For this purpose we introduce the set $\mathbb{E} \in \mathbb{U}$ and the smooth *yield criterion functions* $\hat{\boldsymbol{\Phi}}^\alpha$, $\alpha = 1, \ldots, n$, $\mathbb{U} \to \mathbb{R}$ within the $n + 10$ dimensional space $\mathbb{U} : \mathbb{L}(\mathbb{R}^3, \mathbb{R}^3) \times \mathbb{R}^n \times \mathbb{R}$. We assume that $\mathbb{E}$ is only associated with the *isochoric* stress response of the material. The interior of $\mathbb{E}$ is called the *elastic domain*. It is denoted by $\mathrm{int}(\mathbb{E})$ and defined in the stress space as

$$\mathrm{int}(\mathbb{E}) = \{(\mathrm{dev}\boldsymbol{\Sigma}, \mathbf{a}_0^1, \mathbf{a}_0^2, \ldots, \mathbf{a}_0^n, B) | \hat{\boldsymbol{\Phi}}^\alpha < 0\}, \quad \alpha = 1, \ldots, n \ , \tag{14}$$

where $\mathbb{E}$ is bounded by a convex, but non-smooth, *yield surface* $\partial\mathbb{E}$, defined as

$$\partial\mathbb{E} = \{(\mathrm{dev}\boldsymbol{\Sigma}, \mathbf{a}_0^1, \mathbf{a}_0^2, \ldots, \mathbf{a}_0^n, B) | \hat{\boldsymbol{\Phi}}^\alpha = 0\}, \quad \alpha = 1, \ldots, n \ , \tag{15}$$

and

$$\mathrm{dev}(\bullet) = (\bullet) - \tfrac{1}{3}[(\bullet) : \mathbf{I}]\mathbf{I} \tag{16}$$

denotes the physically correct deviatoric operator in the Eulerian description, where $\mathbf{I}$ is the second–order unit tensor. Note that $\mathbb{E} = \mathrm{int}(\mathbb{E}) \cup \partial\mathbb{E}$. The n-independent (nonredundant) yield criterion functions (introduced in Eqs. (14), (15)) are defined [32]

$$\hat{\boldsymbol{\Phi}}^\alpha = \Phi^\alpha_{\mathrm{macro}}(\mathrm{dev}\boldsymbol{\Sigma}, \mathbf{a}_0^1, \mathbf{a}_0^2, \ldots, \mathbf{a}_0^n) - \Phi_{\mathrm{micro}}(B), \quad \alpha = 1, \ldots, n \ . \tag{17}$$

Note that all states $(\mathrm{dev}\boldsymbol{\Sigma}, \mathbf{a}_0^1, \mathbf{a}_0^2, \ldots, \mathbf{a}_0^n, B) \in \mathbb{U}$ outside $\mathbb{E}$ are non-admissible, and are ruled out.

To describe the plastic deformation of fiber-reinforced composites – in particular, of biological composites – we introduce an active working set $\mathscr{A} = \{\alpha \in 1, \ldots, n | \hat{\boldsymbol{\Phi}}^\alpha = 0\}$ of slip systems. If $\mathscr{A}$ is not equal to the empty set the flow rule determines the way in which plastic deformations evolve; otherwise the deformation is elastic. We propose the following formulation (similar to the description used in crystal plasticity [3, 23, or 28]),

$$\mathbf{L}^{\mathrm{p}} = \sum_{\alpha \in \mathscr{A}} \lambda^\alpha \mathrm{dev}(\mathbf{a}_0^\alpha \otimes \mathbf{a}_0^\alpha) \ , \tag{18}$$

where $\lambda^\alpha \geq 0$ are $n \geq 1$ consistency parameters (slip rates). Hence, the slip system α is active if $\lambda^\alpha > 0$, otherwise it is inactive (for $\lambda^\alpha = 0$). The special flow mechanism provided by the flow rule (18) describes isochoric plastic deformations and incorporates structural information given by the set $\{\mathbf{a}_0^\alpha; \alpha = 1, \ldots, n\}$ of unit vectors. The anisotropic nature of the flow rule is characterized mainly by the same set $\{\mathbf{a}_0^\alpha\}$ of unit vectors, which also characterize, for example, the directions of (collagen) fibers in soft biological tissues.

Remark 2.1. In order to give an interpretation of the introduced flow rule (18) we consider the fiber-reinforced composite, as illustrated schematic in Fig. 1.

We assume to model the composite as a transversely isotropic material with one slip system ($n = 1$). Without loss of generality we assume that the vector $\mathbf{a}_0^1$ coincides with the first Eulerian basis vector $\mathbf{e}_0^1$. Applying a plastic stretch λ^{p} in the direction $\mathbf{a}_0^1$ (see Fig. 1) and using the (plastic) incompressibility condition $J^{\mathrm{p}} = \det \mathbf{F}^{\mathrm{p}} = 1$, the plastic deformation is determined uniquely via the plastic deformation gradient $\mathbf{F}^{\mathrm{p}}$. Thus,

$$[\mathbf{F}^{\mathrm{p}}] = \mathrm{diag}\left[\lambda^{\mathrm{p}}, (\lambda^{\mathrm{p}})^{-1/2}, (\lambda^{\mathrm{p}})^{-1/2}\right] \ , \tag{19}$$

where $[\mathbf{F}^{\mathrm{p}}]$ is a diagonal matrix. Subsequently we use the square brackets $[\bullet]$ for the matrix representation of a second-order tensor. Hence, by means of eq. $(7)_2$, the matrix representation of $\mathbf{L}^{\mathrm{p}}$ follows as

$$[\mathbf{L}^{\mathrm{p}}] = \frac{\dot{\lambda}^{\mathrm{p}}}{\lambda^{\mathrm{p}}} \mathrm{diag}\left[1, -\frac{1}{2}, -\frac{1}{2}\right] = \lambda^1 \left[\mathrm{dev}(\mathbf{a}_0^1 \otimes \mathbf{a}_0^1)\right] \ , \tag{20}$$

with

$$\lambda^1 = \frac{3}{2}\frac{\dot{\lambda}^{\mathrm{p}}}{\lambda^{\mathrm{p}}} \tag{21}$$

(compare with Eq. (18)).

A straightforward generalization of equation (20) to a multislip system leads to the proposed flow rule (18). □

In addition to flow rule (18) we need a rate equation to describe the evolution of the hardening variable A. We postulate that

$$\dot{A} = \sum_{\alpha \in \mathscr{A}} \lambda^\alpha, \quad A|_{t=0} = 0 \ , \tag{22}$$

which is similar to the evolution of the hardening variable in crystal plasticity [32].

In view of the irreversibility of plastic flow the consistency parameters λ^α for each slip system α are assumed to obey the following n (*Karush-Kuhn-Tucker*) loading/unloading conditions

$$\lambda^\alpha \geq 0, \quad \hat{\mathbf{\Phi}}^\alpha \leq 0, \quad \lambda^\alpha \hat{\mathbf{\Phi}}^\alpha = 0, \quad \alpha = 1, \ldots, n \ . \tag{23}$$

In addition to (23), $\lambda^\alpha \geq 0$ satisfy the consistency conditions

$$\lambda^\alpha \dot{\hat{\mathbf{\Phi}}}^\alpha = 0, \quad \alpha = 1, \ldots, n \ . \tag{24}$$

The introduction of this efficient concept allows a distinction to be made between different modes of the material response. We deduce the mathematical representation

$$\begin{aligned}
&\hat{\mathbf{\Phi}}^\alpha < 0, \ \alpha = 1, \ldots, n \Leftrightarrow (\bullet) \in \mathrm{int}(\mathbb{E}) \\
&\quad \Rightarrow \lambda^\alpha = 0 \text{ elastic response,} \\
&\hat{\mathbf{\Phi}}^\alpha = 0, \ \alpha = 1, \ldots, n \\
&\quad \Leftrightarrow (\bullet) \in \partial\mathbb{E} \begin{cases} \dot{\hat{\mathbf{\Phi}}}^\alpha < 0 \ \Rightarrow \ \lambda^\alpha = 0 & \text{elastic unloading,} \\ \dot{\hat{\mathbf{\Phi}}}^\alpha = 0 \text{ and } \lambda^\alpha = 0 & \text{neutral loading,} \\ \dot{\hat{\mathbf{\Phi}}}^\alpha = 0 \text{ and } \lambda^\alpha > 0 & \text{plastic loading,} \end{cases}
\end{aligned}$$

where $(\bullet)$ denotes a convenient short-hand notation for any $(\mathrm{dev}\boldsymbol{\Sigma}, \mathbf{a}_0^1, \mathbf{a}_0^2, \ldots, \mathbf{a}_0^n, B)$.

The set of Eqs. (17, 18, 22–24) describes the evolution of rate-independent anisotropic plastic flow. The continuum mechanical framework is summarized in Box 1.

Before we provide the numerical recipes suitable for a finite element implementation, the two functions Φ_{macro} and Φ_{micro} introduced in (17) require a specification. This specification, given in the subsequent section, must be in agreement with experimental investigations on the matter of interest.

2.4 Model Problem. Multislip soft fiber-reinforced composite

In this section we particularize the continuum mechanical formulation of finite strain multisurface plasticity introduced above to soft fiber-reinforced composites. We restrict the following investigation to (nearly) incompressible soft biological tissues, in particular to blood vessels which are capable of supporting finite plastic strains in the high internal pressure domain [40].

Box 1. Continuum mechanical description of multisurface plasticity

Anisotropic free-energy function:

$$\Psi(\mathbf{F}^{\mathrm{e}}, \mathbf{a}_0^1, \mathbf{a}_0^2, \ldots, \mathbf{a}_0^n, A) = \Psi_{\mathrm{macro}}(\mathbf{F}^{\mathrm{e}}, \mathbf{a}_0^1, \mathbf{a}_0^2, \ldots, \mathbf{a}_0^n) + \Psi_{\mathrm{micro}}(A)$$

Anisotropic yield criterion functions:

$$\hat{\mathbf{\Phi}}^\alpha = \Phi^\alpha_{\mathrm{macro}}(\mathrm{dev}\boldsymbol{\Sigma}, \mathbf{a}_0^1, \mathbf{a}_0^2, \ldots, \mathbf{a}_0^n) - \Phi_{\mathrm{micro}}(B), \quad \alpha = 1, \ldots, n$$

Anisotropic flow rule:

$$\mathbf{L}^{\mathrm{p}} = \sum_{\alpha \in \mathscr{A}} \lambda^\alpha \mathrm{dev}\left(\mathbf{a}_0^\alpha \otimes \mathbf{a}_0^\alpha\right)$$

Evolution of the hardening variable A:

$$\dot{A} = \sum_{\alpha \in \mathscr{A}} \lambda^\alpha, \quad A|_{t=0} = 0$$

Karush-Kuhn-Tucker loading/unloading conditions:

$$\lambda^\alpha \geq 0, \quad \hat{\mathbf{\Phi}}^\alpha \leq 0, \quad \lambda^\alpha \hat{\mathbf{\Phi}}^\alpha = 0, \quad \alpha = 1, \ldots, n$$

Consistency conditions:

$$\lambda^\alpha \dot{\hat{\mathbf{\Phi}}}^\alpha = 0, \quad \alpha = 1, \ldots, n$$

2.4.1 Anisotropic elastic response

(i) Free-energy function. In order to describe (nearly) incompressible response, we use the following representation of the macroscopic free-energy function

$$\Psi_{\mathrm{macro}}(\mathbf{F}^{\mathrm{e}}, \mathbf{a}_0^1, \ldots, \mathbf{a}_0^n) = L(J) + \bar{\Psi}(\bar{\mathbf{F}}^{\mathrm{e}}, \mathbf{a}_0^1, \ldots, \mathbf{a}_0^n) \ , \tag{25}$$

where J and $\bar{\mathbf{F}}^{\mathrm{e}}$ are the volume ratio and the modified elastic deformation gradient, respectively.

The first part $L(J)$ on the right-hand side of Eq. (25) characterizes a scalar-valued function – with the property $L(1) = 0$ – which is motivated mathematically. It serves as a penalty function enforcing the incompressibility constraint [4]. The second part $\bar{\Psi}(\bar{\mathbf{F}}^{\mathrm{e}}, \mathbf{a}_0^1, \ldots, \mathbf{a}_0^n)$ is the energy stored in the tissue when it is subjected to isochoric elastic deformations characterized by $\bar{\mathbf{F}}^{\mathrm{e}}$. The anisotropic structure of this potential is described in terms of the set $\{\mathbf{a}_0^\alpha; \alpha = 1, \ldots, n\}$ of unit vectors.

Based on the theory of fiber-reinforced composites [19, 20, 54], an additive split of $\bar{\Psi}$ is postulated according to

$$\bar{\Psi}(\bar{\mathbf{F}}^{\mathrm{e}}, \mathbf{a}_0^1, \ldots, \mathbf{a}_0^n) = \bar{\Psi}_{\mathrm{gs}}(\bar{\mathbf{F}}^{\mathrm{e}}) + \bar{\Psi}_{\mathrm{f}}(\bar{\mathbf{F}}^{\mathrm{e}}, \mathbf{a}_0^1, \ldots, \mathbf{a}_0^n) \ . \tag{26}$$

Here the potential $\bar{\Psi}_{\mathrm{gs}}$ models the (isotropic) matrix material (subsequently identified by the subscript $(\bullet)_{\mathrm{gs}}$), while $\bar{\Psi}_{\mathrm{f}}$ incorporates the anisotropic behavior due to the fiber reinforcement, i.e. collagen-fibers (identified by $(\bullet)_{\mathrm{f}}$). For a histomechanical motivation for introduction of the split (26) the reader is referred to [21].

(ii) Elastic stress response. From the macroscopic free-energy function (25) the Kirchhoff stress tensor $\boldsymbol{\tau}$ can be derived in a standard way. Its decoupled representation is given by

$$\boldsymbol{\tau}(\mathbf{F}^{\mathrm{e}}, \mathbf{a}_0^1, \ldots, \mathbf{a}_0^n) = 2\frac{\partial \Psi_{\mathrm{macro}}(\mathbf{F}^{\mathrm{e}}, \mathbf{a}_0^1, \ldots, \mathbf{a}_0^n)}{\partial \mathbf{g}} = \boldsymbol{\tau}_{\mathrm{L}} + \tilde{\boldsymbol{\tau}} \ , \tag{27}$$

$$\boldsymbol{\tau}_{\mathrm{L}} = 2\frac{\partial L(J)}{\partial \mathbf{g}}, \quad \tilde{\boldsymbol{\tau}} = 2\frac{\partial \bar{\Psi}(\bar{\mathbf{F}}^{\mathrm{e}}, \mathbf{a}_0^1, \ldots, \mathbf{a}_0^n)}{\partial \mathbf{g}} \ , \tag{28}$$

where $\tilde{\boldsymbol{\tau}}$ denotes the isochoric Kirchhoff stress tensor, while the stresses $\boldsymbol{\tau}_{\mathrm{L}}$ enforce the incompressibility constraint.

2.4.2
Anisotropic inelastic response

Here we specify the set of equations necessary to describe the inelastic response of soft biological tissues. The associated continuum basis is given in Sect. 2.3.

In order to provide the n-independent yield criterion functions (17) we particularize the macro-stress dependent functions $\Phi^{\alpha}_{\mathrm{macro}}$, $\alpha = 1, \ldots, n$, in such a way that we omit coupling effects between the different slip systems. Therefore, we introduce new functions, which we denote by τ^{α}, $\alpha = 1, \ldots, n$. It is assumed that these functions are the projections of the deviatoric Mandel stress tensor onto the particular slip system $\mathbf{a}_0^{\alpha}$, i.e.

$$\begin{aligned}\Phi^{\alpha}_{\mathrm{macro}}(\mathrm{dev}\boldsymbol{\Sigma}, \mathbf{a}_0^1, \mathbf{a}_0^2, \ldots, \mathbf{a}_0^n) &= \tau^{\alpha}(\ \mathrm{dev}\boldsymbol{\Sigma}, \mathbf{a}_0^{\alpha}) \\ &= \mathrm{dev}\boldsymbol{\Sigma} : \mathbf{a}_0^{\alpha} \otimes \mathbf{a}_0^{\alpha} \ ,\end{aligned} \tag{29}$$

which is similar to the definition of the *Schmid* resolved shear stresses in crystal plasticity [23, 28, 32].

Based on isotropic Taylor hardening [29], we assume that the micro-stress dependent function Φ_{micro}, introduced in Eq. (17), can be additively decomposed into an initial yield stress τ_0 and a micro-stress B. We adopt the common concepts of linear and exponential hardening, which are based on a three parameter model [50], and write

$$\begin{aligned}&\Phi_{\mathrm{micro}}(B) = \tau_0 + B, \\ &B = hA + \tau_{0,\infty}\left[1 - \exp\left(-\frac{A}{a_0}\right)\right] \ ,\end{aligned} \tag{30}$$

where hardening is described by the linear hardening parameter h and the nonlinear hardening parameters $\tau_{0,\infty}$ and a_0.

Using Eqs. (29) and (30), the yield criterion functions (17) have the specific form

$$\hat{\Phi}^{\alpha} = \tau^{\alpha} - (\tau_0 + B), \quad \alpha = 1, \ldots, n \ . \tag{31}$$

All that remains is to particularize the crucial free-energy function Ψ_{macro}, which is the aim of the next section.

2.4.3
Particularization of the model problem for arteries

(i) Free-energy function. In order to characterize the mechanical behavior of arteries we choose a formulation of the macroscopic free-energy function (25) which is based on the theory of invariants [54]. With the aim of minimizing the number of material parameters we propose the representation

$$\Psi_{\mathrm{macro}}(\mathbf{F}^{\mathrm{e}}, \mathbf{a}_0^1, \ldots, \mathbf{a}_0^n) = L(J) + \bar{\Psi}_{\mathrm{gs}}(\bar{I}_1) + \sum_{\alpha \in \mathscr{B}} \bar{\Psi}^{\alpha}_{\mathrm{f}}(\bar{I}^{\alpha}_4) \ , \tag{32}$$

where $\bar{I}_1 = \mathrm{tr}\bar{\mathbf{C}}^{\mathrm{e}}$ is the first invariant of the modified elastic right Cauchy-Green tensor $\bar{\mathbf{C}}^{\mathrm{e}}$, which is well-known from the isotropic theory, and $\bar{I}^{\alpha}_4$ are additional invariants of $\bar{\mathbf{C}}^{\mathrm{e}}$ and the structural tensors $\mathbf{a}_0^{\alpha} \otimes \mathbf{a}_0^{\alpha}$, given by

$$\bar{I}^{\alpha}_4 = \bar{\mathbf{C}}^{\mathrm{e}} : \mathbf{a}_0^{\alpha} \otimes \mathbf{a}_0^{\alpha}, \quad \alpha = 1, \ldots, n \tag{33}$$

(compare also with [19–21, 54]). Note that for the incompressible limit ($J = 1$) we have $\bar{\mathbf{C}}^{\mathrm{e}} = \mathbf{C}^{\mathrm{e}}$, and Eq. (33) reads $\bar{I}^{\alpha}_4 = \mathbf{C}^{\mathrm{e}} : \mathbf{a}_0^{\alpha} \otimes \mathbf{a}_0^{\alpha}$.

We assume that the fibers do not carry any compressive load. In Eq. (32), this situation is expressed by the set $\mathscr{B} = \{\alpha \in 1, \ldots, n | \bar{I}^{\alpha}_4 > 1\}$ of active fibers which are stretched. Only these active fibers contribute to the free-energy function Ψ_{macro}. Note that for an incompressible material the invariants $\bar{I}^{\alpha}_4$ can be identified with the square of the elastic stretch in the direction of the α-th family of fibers [19].

Finally, we postulate that the three parts of the free energy (32) have the forms

$$L(J) = \frac{\kappa}{2}(J-1)^2, \quad \bar{\Psi}_{\mathrm{gs}}(\bar{I}_1) = \frac{\mu}{2}(\bar{I}_1 - 3) \ , \tag{34}$$

$$\bar{\Psi}^{\alpha}_{\mathrm{f}}(\bar{I}^{\alpha}_4) = \frac{k_1}{2k_2}\left\{\exp\left[k_2\left(\bar{I}^{\alpha}_4 - 1\right)^2\right] - 1\right\}, \quad \alpha = 1, \ldots, n \ , \tag{35}$$

which are well-suited for the description of the anisotropic mechanical behavior of arterial walls during typical (physiological) loading conditions. Here the material parameter μ describes the isotropic response, while k_1 and k_2 are associated with the anisotropic material behavior. The parameter κ serves as a user–specified *penalty* parameter which has no physical relevance (for $\kappa \to \infty$, expression (32) may be viewed as the potential for the incompressible limit, with $J = 1$). Note that for the function $\bar{\Psi}_{\mathrm{gs}}$ we may apply any Ogden-type elastic material [38].

We assume that each family of fibers has the same mechanical response, which implies that k_1 and k_2 are the same for each fiber family. In fact, $\bar{\Psi}^{\alpha}_{\mathrm{f}}$ describes the energy stored in the α-th family of fibers. Note that only two families of fibers (expressed through the invariants $\bar{I}^{\alpha}_4$, $\alpha = 1, 2$) are necessary to capture the typical features of elastic arterial response [21].

The energy functions (34), (35) do not incorporate coupling phenomena occurring between the n families of fibers. To incorporate coupling effects a more general constitutive approach is required [20] and various experiments are needed to identify the increasing number of material parameters.

The energy functions (34), (35) are quite different from the well-known strain-energy function for arteries proposed by Fung [16]. An advantage of the proposed constitutive model is the fact that the material parameters involved may be associated partly with the histological structure of the arterial wall, which is not possible with the purely phenomenological model by *Fung*. However, the

anisotropic contribution (35) to the proposed free energy Ψ_{macro} is able to replicate the basic characteristic of the potential by Fung. A comparative study which investigates the two different potentials is given in [21].

For further use in this study we introduce the set $\{\mathbf{a}^\alpha; \alpha = 1, \dots, n\}$ of Eulerian vectors $\mathbf{a}^\alpha$. They are defined as maps of the structural measures $\mathbf{a}_0^\alpha$ via the unimodular elastic part $\bar{\mathbf{F}}^{\mathrm{e}}$ of the deformation gradient, according to

$$\mathbf{a}^\alpha = \bar{\mathbf{F}}^{\mathrm{e}} \mathbf{a}_0^\alpha, \quad \alpha = 1, \dots, n \ . \tag{36}$$

In addition, we introduce two symmetric $n \times n$ matrices through the dot products of the Eulerian vectors $\mathbf{a}^\alpha$, and the Lagrangian vectors $\mathbf{a}_0^\alpha$, according to

$$a^{\alpha\beta} = \mathbf{a}^\alpha \cdot \mathbf{a}^\beta, \quad A^{\alpha\beta} = \mathbf{a}_0^\alpha \cdot \mathbf{a}_0^\beta, \quad \alpha, \beta = 1, \dots, n \ . \tag{37}$$

Note that the diagonal terms $A^{\alpha\alpha}$ take on the values 1, since $\mathbf{a}_0^\alpha$ are unit vectors.

Using the definitions (36) of the Eulerian vectors $\mathbf{a}^\alpha$ and relation $(37)_1$ for the matrices $a^{\alpha\beta}$, the invariants $\bar{I}_4^\alpha$ can also be expressed as

$$\bar{I}_4^\alpha = \mathbf{a}^\alpha \cdot \mathbf{a}^\alpha = a^{\alpha\alpha}, \quad \alpha = 1, \dots, n \ , \tag{38}$$

which may be shown immediately using Eq. (33) and by means of the index notation. Hence, we conclude that the diagonal terms $a^{\alpha\alpha}$ are the invariants $\bar{I}_4^\alpha$.

Remark 2.2. The invariant $\bar{I}_1$ can be expressed in a similar way to the invariants $\bar{I}_4^\alpha$. By use of the spectral decomposition of the (second-order) unit tensor $\mathbf{I} = \sum_{i=1}^3 \mathbf{e}_0^i \otimes \mathbf{e}_0^i$, we may write

$$\bar{I}_1 = \mathrm{tr}\bar{\mathbf{C}}^{\mathrm{e}} = \bar{\mathbf{C}}^{\mathrm{e}} : \mathbf{I} = \bar{\mathbf{C}}^{\mathrm{e}} : \sum_{i=1}^3 \mathbf{e}_0^i \otimes \mathbf{e}_0^i = \sum_{i=1}^3 \mathbf{e}^i \cdot \mathbf{e}^i \ . \tag{39}$$

Here we have mapped the Lagrangian basis vectors $\mathbf{e}_0^i$, $i = 1, 2, 3$, using the unimodular part of the elastic deformation gradient $\bar{\mathbf{F}}^{\mathrm{e}}$, and we have introduced the relation

$$\mathbf{e}^i = \bar{\mathbf{F}}^{\mathrm{e}} \mathbf{e}_0^i, \quad i = 1, 2, 3 \ . \tag{40}$$

Note that the vectors $\mathbf{e}^i$, $i = 1, 2, 3$, should not be confused with the Eulerian basis vectors. □

(ii) Elastic stress response. From the macroscopic free-energy function (32) we may derive the associated Kirchhoff stress tensor. By means of the physical expression $(27)_1$ we obtain

$$\boldsymbol{\tau} = \boldsymbol{\tau}_{\mathrm{L}} + \tilde{\boldsymbol{\tau}}, \ \ \tilde{\boldsymbol{\tau}} = \tilde{\boldsymbol{\tau}}_{\mathrm{gs}} + \sum_{\alpha \in \mathscr{B}} \tilde{\boldsymbol{\tau}}_{\mathrm{f}}^\alpha \ , \tag{41}$$

with the explicit expressions $\boldsymbol{\tau}_{\mathrm{L}} = 2\partial L(J)/\partial \mathbf{g}$ and $\tilde{\boldsymbol{\tau}}_{\mathrm{gs}} = 2\partial \bar{\boldsymbol{\Psi}}_{\mathrm{gs}}(\bar{I}_1)/\partial \mathbf{g}$, $\tilde{\boldsymbol{\tau}}_{\mathrm{f}}^\alpha = 2\partial \bar{\boldsymbol{\Psi}}_{\mathrm{f}}^\alpha(\bar{I}_4^\alpha)/\partial \mathbf{g}$, $\alpha = 1, \dots, n$, for the Kirchhoff stress response. Successive application of the chain rule gives

$$\boldsymbol{\tau}_{\mathrm{L}} = 2\frac{\partial L(J)}{\partial J}\frac{\partial J}{\partial \mathbf{C}^{\mathrm{e}}} : \frac{\partial \mathbf{C}^{\mathrm{e}}}{\partial \mathbf{g}}, \ \ \tilde{\boldsymbol{\tau}}_{\mathrm{gs}} = 2\frac{\partial \bar{\boldsymbol{\Psi}}_{\mathrm{gs}}(\bar{I}_1)}{\partial \bar{\mathbf{C}}^{\mathrm{e}}} : \frac{\partial \bar{\mathbf{C}}^{\mathrm{e}}}{\partial \mathbf{C}^{\mathrm{e}}} : \frac{\partial \mathbf{C}^{\mathrm{e}}}{\partial \mathbf{g}} \ , \tag{42}$$

$$\tilde{\boldsymbol{\tau}}_{\mathrm{f}}^\alpha = 2\frac{\partial \bar{\boldsymbol{\Psi}}_{\mathrm{f}}(\bar{I}_4^\alpha)}{\partial \bar{\mathbf{C}}^{\mathrm{e}}} : \frac{\partial \bar{\mathbf{C}}^{\mathrm{e}}}{\partial \mathbf{C}^{\mathrm{e}}} : \frac{\partial \mathbf{C}^{\mathrm{e}}}{\partial \mathbf{g}}, \quad \alpha = 1, \dots, n \ . \tag{43}$$

In Eqs. (42), (43), the partial derivatives $\partial J/\partial \mathbf{C}^{\mathrm{e}}$ and $\partial \bar{\mathbf{C}}^{\mathrm{e}}/\partial \mathbf{C}^{\mathrm{e}}$ take on the forms [19]

$$\frac{\partial J}{\partial \mathbf{C}^{\mathrm{e}}} = \frac{1}{2} J \mathbf{C}^{\mathrm{e}-1}, \ \ \frac{\partial \bar{\mathbf{C}}^{\mathrm{e}}}{\partial \mathbf{C}^{\mathrm{e}}} = J^{-2/3}\left(\mathbb{I} - \frac{1}{3}\bar{\mathbf{C}}^{\mathrm{e}} \otimes \bar{\mathbf{C}}^{\mathrm{e}-1}\right), \tag{44}$$

where the fourth-order unit tensor $\mathbb{I}$ is governed by the rule $(\mathbb{I})_{IJKL} = (\delta_{IK}\delta_{JL} + \delta_{IL}\delta_{JK})/2$.

An additional result needed in the computation of the stress response is the partial derivative of the elastic right Cauchy-Green tensor $\mathbf{C}^{\mathrm{e}}$ with respect to the Eulerian metric tensor $\mathbf{g}$. For that we use the more general expression $\mathbf{C}^{\mathrm{e}} = \mathbf{F}^{\mathrm{e}\mathrm{T}}\mathbf{g}\mathbf{F}^{\mathrm{e}}$ of the elastic right Cauchy-Green tensor, defined as a pull-back operation of $\mathbf{g}$ (note that by means of a rectangular coordinate system, in which $\mathbf{g} = \mathbf{I}$, this expression reduces to $\mathbf{C}^{\mathrm{e}} = \mathbf{F}^{\mathrm{e}\mathrm{T}}\mathbf{F}^{\mathrm{e}}$). Hence, we find by means of the chain rule and index notation that

$$\frac{\partial (F_{aK}^{\mathrm{e}} g_{ab} F_{bL}^{\mathrm{e}})}{\partial g_{ij}} = F_{aK}^{\mathrm{e}} (\mathbb{I})_{abij} F_{bL}^{\mathrm{e}} = \tfrac{1}{2}(F_{iK}^{\mathrm{e}} F_{jL}^{\mathrm{e}} + F_{jK}^{\mathrm{e}} F_{iL}^{\mathrm{e}}) \ , \tag{45}$$

which is only valid for Cartesian coordinates. Equation (45) reads in symbolic notation

$$\frac{\partial \mathbf{C}^{\mathrm{e}}}{\partial \mathbf{g}} = \mathbf{F}^{\mathrm{e}} \odot \mathbf{F}^{\mathrm{e}}$$

with

$$(\mathbf{F}^{\mathrm{e}} \odot \mathbf{F}^{\mathrm{e}})_{ijKL} = \frac{1}{2}(F_{iK}^{\mathrm{e}} F_{jL}^{\mathrm{e}} + F_{jK}^{\mathrm{e}} F_{iL}^{\mathrm{e}}) \ , \tag{46}$$

where $\mathbf{F}^{\mathrm{e}} \odot \mathbf{F}^{\mathrm{e}}$ defines a tensor product governed by the rule $(46)_2$. For notational convenience, in this paper we do not distinguish between co- and contravariant tensors and accept therefore the abuse of notation introduced in Eq. (45).

Using the expressions (42), (43) for the Kirchhoff stress tensors, the properties (44), (46) and the specified free-energy functions (34), (35), we find that the elastic stress response is governed by the three contributions

$$\boldsymbol{\tau}_{\mathrm{L}} = Jp\mathbf{I}, \quad \tilde{\boldsymbol{\tau}}_{\mathrm{gs}} = \mu \, \mathrm{dev}\, \bar{\mathbf{b}}^{\mathrm{e}},$$
$$\tilde{\boldsymbol{\tau}}_{\mathrm{f}}^\alpha = 2\psi^\alpha \mathrm{dev}(\mathbf{a}^\alpha \otimes \mathbf{a}^\alpha), \quad \alpha \in \mathscr{B} \ . \tag{47}$$

Here we have used the definitions

$$p = \frac{\mathrm{d}L(J)}{\mathrm{d}J}, \quad \psi^\alpha = \frac{\mathrm{d}\bar{\Psi}_{\mathrm{f}}^\alpha(\bar{I}_4^\alpha)}{\mathrm{d}\bar{I}_4^\alpha} \tag{48}$$

of the hydrostatic pressure p and the stress functions ψ^α with the specified forms

$$p = \kappa(J-1), \quad \psi^\alpha = k_1(\bar{I}_4^\alpha - 1)\exp[k_2(\bar{I}_4^\alpha - 1)^2] \ . \tag{49}$$

For an explicit derivation of the isochoric stress response associated with $\bar{\boldsymbol{\Psi}}_{\mathrm{f}}^\alpha$, the reader is referred to Appendix A.1.

(iii) Inelastic stress response. The aim now is to specify the Mandel stress tensor $\boldsymbol{\Sigma}$ with respect to relation $(8)_2$. By

means of the explicit expressions (41), (47) for the Kirchhoff stress tensor $\boldsymbol{\tau}$, the definitions $\bar{\mathbf{C}}^{\mathrm{e}} = \bar{\mathbf{F}}^{\mathrm{eT}}\bar{\mathbf{F}}^{\mathrm{e}}$, $\bar{\mathbf{b}}^{\mathrm{e}} = \bar{\mathbf{F}}^{\mathrm{e}}\bar{\mathbf{F}}^{\mathrm{eT}}$ and the definition $\mathbf{a}^{\alpha} = \bar{\mathbf{F}}^{\mathrm{e}}\mathbf{a}_0^{\alpha}$ of the Eulerian vectors, we find that

$$\boldsymbol{\Sigma} = Jp\mathbf{I} + \mu\,\mathrm{dev}\,\bar{\mathbf{C}}^{\mathrm{e}} + 2\sum_{\beta\in\mathscr{B}}\psi^{\beta}\;\mathrm{dev}(\bar{\mathbf{C}}^{\mathrm{e}}\mathbf{a}_0^{\beta}\otimes\mathbf{a}_0^{\beta})\;. \qquad (50)$$

Hence, we substitute Eq. (50) into $(29)_2$ and take advantage of property (16). Using the definitions $\bar{I}_1 = \mathrm{tr}\bar{\mathbf{C}}^{\mathrm{e}}$, $\bar{I}_4^{\alpha} = \bar{\mathbf{C}}^{\mathrm{e}} : \mathbf{a}_0^{\alpha}\otimes\mathbf{a}_0^{\alpha}$ of the invariants and the properties $\mathbf{I} : \mathbf{a}_0^{\alpha}\otimes\mathbf{a}_0^{\alpha} = 1$ and $\bar{\mathbf{C}}^{\mathrm{e}}\mathbf{a}_0^{\alpha}\otimes\mathbf{a}_0^{\alpha} : \mathbf{a}_0^{\beta}\otimes\mathbf{a}_0^{\beta} = A^{\alpha\beta}a^{\alpha\beta}$ (recall the definitions (37) of the symmetric $n\times n$ matrices $A^{\alpha\beta}$ and $a^{\alpha\beta}$), we find the scalar measures τ^{α} of the stress state, i.e.

$$\tau^{\alpha} = \mu\left(\bar{I}_4^{\alpha} - \frac{1}{3}\bar{I}_1\right) + 2\sum_{\beta\in\mathscr{B}}\psi^{\beta}\left(A^{\alpha\beta}a^{\alpha\beta} - \frac{1}{3}\bar{I}_4^{\beta}\right), \qquad \alpha = 1,\ldots,n\;. \qquad (51)$$

It turns out that within a finite element implementation, the relation (51) plays a crucial role. Although the structure of Eq. (51) is simple, this equation requires substantial numerical effort to be solved.

(iv) Plastic dissipation. With Eqs. $(13)_2$, (18), (50) and the rate equation (22), the plastic dissipation of the model is given as

$$\mathscr{D}^{\mathrm{p}} = \mu\sum_{\alpha\in\mathscr{A}}\lambda^{\alpha}\left(\bar{I}_4^{\alpha} - \frac{1}{3}\bar{I}_1\right) + 2\sum_{\alpha\in\mathscr{A}}\sum_{\beta\in\mathscr{B}}\psi^{\beta}\lambda^{\alpha} \times\left(A^{\alpha\beta}a^{\alpha\beta} - \frac{1}{3}\bar{I}_4^{\beta}\right) - B\sum_{\alpha\in\mathscr{A}}\lambda^{\alpha} \geq 0 \qquad (52)$$

(the derivation is analogous to the procedure which led to Eq. (51)). We suppose that the states $\{\mathrm{dev}\boldsymbol{\Sigma}, \mathbf{a}_0^1, \mathbf{a}_0^2, \ldots, \mathbf{a}_0^n, B\} \in \partial\mathbb{E}$ which, in view of (15), implies that $\dot{\hat{\boldsymbol{\Phi}}} = 0$. With use of (51) and rate equation (22) we may rewrite the plastic dissipation (52) in the remarkably simple form

$$\mathscr{D}^{\mathrm{p}} = \sum_{\alpha\in\mathscr{A}}\lambda^{\alpha}(\tau^{\alpha} - B) = \tau_0\dot{A} \geq 0\;. \qquad (53)$$

We conclude from Eq. (22) and the *Karush-Kuhn-Tucker* loading/unloading conditions (23) that the time derivative $\dot{A} \geq 0$ of the hardening parameter is non-negative. Hence, the non-negativity of the plastic dissipation $\mathscr{D}^{\mathrm{p}}$ is ensured.

Note that the simple form (53) does not consider plastic dissipation due to hardening effects, which means that the power associated with hardening effects is stored completely in the material. In the event that experimental studies do not confirm this assumption additional internal variables can be introduced.

The continuum mechanical part of the material model is now described completely. The numerical recipes necessary for an efficient finite element implementation are derived in the next section.

3
Integration of the evolution equations

In this section we derive the algebraic expressions necessary for use of our material model within approximation techniques such as the finite element method. For this purpose we apply an established integration scheme drawn from computational mechanics. It is based on the unconditionally stable backward-Euler integration of the continuous evolution equations and the elastic predictor/plastic corrector concept [50]. This efficient concept embraces an iterative update of Newton's type of the Eulerian vectors (see [32]), $\mathbf{a}^{\alpha} = \bar{\mathbf{F}}^{\mathrm{e}}\mathbf{a}_0^{\alpha}$, $\alpha = 1,\ldots,n$, and $\mathbf{e}^{i} = \bar{\mathbf{F}}^{\mathrm{e}}\mathbf{e}_0^{i}$, $i = 1,2,3$, defined in Eqs. (36) and (40), respectively.

3.1
Backward-Euler integration of the evolution equations and Eulerian vector updates

Consider a partition $\bigcup_{n=0}^{M}[t_n, t_{n+1}]$ of the closed time interval $t\in[0,T]$, where $0 = t_0 < \cdots < t_{M+1} = T$ and $M+1$ is the number of all time sub-intervals. We focus attention on a typical sub-interval $[t_n, t_{n+1}]$ and assume that the plastic part $\mathbf{F}_n^{\mathrm{p}}$ of the deformation gradient (consequently $\mathbf{F}_n^{\mathrm{p}-1}$), and the hardening variable A_n are known at time t_n. The backward-Euler discretization of $\mathbf{L}^{\mathrm{p}}$ (see Eq. $(7)_2$) reads,

$$\mathbf{L}_{n+1}^{\mathrm{p}}\Delta t = \mathbf{I} - \mathbf{F}_n^{\mathrm{p}}\mathbf{F}_{n+1}^{\mathrm{p}-1}\;, \qquad (54)$$

where $\Delta t = t_{n+1} - t_n$ denotes a given time increment (for convenience, we will not indicate subsequently the subscript $n+1$). Substitution of the specific flow rule (18) in (54) gives

$$\sum_{\alpha\in\mathscr{A}}\gamma^{\alpha}\mathrm{dev}(\mathbf{a}_0^{\alpha}\otimes\mathbf{a}_0^{\alpha}) = \mathbf{I} - \mathbf{F}_n^{\mathrm{p}}\mathbf{F}^{\mathrm{p}-1}\;, \qquad (55)$$

where $\gamma^{\alpha} := \lambda^{\alpha}\Delta t$ denote the *incremental* slip (plastic) parameters on each slip system α. Based on these definitions and the use of Eqs. (23) and (24) the incremental *Karush-Kuhn-Tucker* conditions and the incremental consistency conditions read,

$$\gamma^{\alpha} \geq 0,\;\; \hat{\boldsymbol{\Phi}}^{\alpha} \leq 0,\;\; \gamma^{\alpha}\hat{\boldsymbol{\Phi}}^{\alpha} = 0,\;\; \gamma^{\alpha}\dot{\hat{\boldsymbol{\Phi}}}^{\alpha} = 0, \qquad \alpha = 1,\ldots,n\;. \qquad (56)$$

In order to find an update formula for the unimodular part $\bar{\mathbf{F}}^{\mathrm{e}}$ of the elastic deformation gradient, which is suitable for numerical implementation, we multiply (55) by $\mathbf{F}\mathbf{F}_n^{\mathrm{p}-1}$ on the left hand-side. With the assumptions $J^{\mathrm{e}} = J$, $J^{\mathrm{p}} = 1$ and the definitions $\mathbf{F} = \mathbf{F}^{\mathrm{e}}\mathbf{F}^{\mathrm{p}}$, $\mathbf{F}^{\mathrm{e}} = J^{1/3}\bar{\mathbf{F}}^{\mathrm{e}}$ and $\mathbf{F}^{\mathrm{p}} = \bar{\mathbf{F}}^{\mathrm{p}}$ introduced in Eqs. (1), $(2)_1$ and $(2)_3$, the relation (55) leads, after some standard algebraic manipulations, to

$$\bar{\mathbf{F}}^{\mathrm{e}} = \bar{\mathbf{F}}^{\mathrm{e\,tr}} - \sum_{\alpha\in\mathscr{A}}\gamma^{\alpha}\left(\mathbf{a}^{\alpha\,\mathrm{tr}}\otimes\mathbf{a}_0^{\alpha} - \frac{1}{3}\bar{\mathbf{F}}^{\mathrm{e\,tr}}\right)\;. \qquad (57)$$

In what follows, the notation $(\bullet)^{\mathrm{tr}}$ indicates *elastic trial* (*predictor*) state values which are achieved by freezing the plastic deformation (for further details see, for example, [32, 50]). For Eq. (57) we introduced the definitions

$$\bar{\mathbf{F}}^{\mathrm{e\,tr}} = \bar{\mathbf{F}}\bar{\mathbf{F}}_n^{\mathrm{p}-1} \;\text{ and }\; \mathbf{a}^{\alpha\,\mathrm{tr}} = \bar{\mathbf{F}}^{\mathrm{e\,tr}}\mathbf{a}_0^{\alpha}, \quad \alpha\in\mathscr{A}\cup\mathscr{B} \qquad (58)$$

of the trial quantities and $\mathscr{A} \cup \mathscr{B}$ denotes the union of the active working set and the set of stretched fibers. The update formula of the hardening variable A is obtained immediately by discretization of Eq. (22), i.e.

$$A = A^{\mathrm{tr}} + \sum_{\alpha \in \mathscr{A}} \gamma^{\alpha}, \quad A^{\mathrm{tr}} = A_n \ . \tag{59}$$

Using Eqs. (36) and (57) and the definitions $(58)_2$ of $\mathbf{a}^{\alpha\,\mathrm{tr}}$ and $(37)_2$ of $A^{\alpha\beta}$, the update formulas for the Eulerian vectors $\mathbf{a}^{\alpha}$ read

$$\begin{aligned}\mathbf{a}^{\alpha} &= \mathbf{a}^{\alpha\,\mathrm{tr}} - \sum_{\beta \in \mathscr{A}} \gamma^{\beta} \left(\mathbf{a}^{\beta\,\mathrm{tr}} A^{\alpha\beta} - \frac{1}{3} \mathbf{a}^{\alpha\,\mathrm{tr}} \right) \\ &= \mathbf{a}^{\alpha\,\mathrm{tr}} \left(1 + \frac{1}{3} \sum_{\beta \in \mathscr{A}} \gamma^{\beta} \right) - \sum_{\beta \in \mathscr{A}} \gamma^{\beta} \mathbf{a}^{\beta\,\mathrm{tr}} A^{\alpha\beta}, \quad \alpha \in \mathscr{A} \cup \mathscr{B} \ .\end{aligned} \tag{60}$$

Similarly, on use of Eqs. (40) and (57) and the definition of the trial vectors $\mathbf{e}^{i\,\mathrm{tr}} = \bar{\mathbf{F}}^{\mathrm{e}\,\mathrm{tr}} \mathbf{e}_0^i$, we obtain the update formulas

$$\begin{aligned}\mathbf{e}^{i} &= \mathbf{e}^{i\,\mathrm{tr}} - \sum_{\beta \in \mathscr{A}} \gamma^{\beta} \left(\mathbf{a}^{\beta\,\mathrm{tr}} B^{i\beta} - \frac{1}{3} \mathbf{e}^{i\,\mathrm{tr}} \right) \\ &= \mathbf{e}^{i\,\mathrm{tr}} \left(1 + \frac{1}{3} \sum_{\beta \in \mathscr{A}} \gamma^{\beta} \right) - \sum_{\beta \in \mathscr{A}} \gamma^{\beta} \mathbf{a}^{\beta\,\mathrm{tr}} B^{i\beta}, \quad i = 1,2,3\end{aligned} \tag{61}$$

for the Eulerian vectors $\mathbf{e}^i$, $i = 1,2,3$. By analogy with eq. $(37)_2$ we have introduced the constant $n \times 3$ matrices $B^{\alpha i} = \mathbf{a}_0^{\alpha} \cdot \mathbf{e}_0^i$.

3.2
Computation of the incremental slip parameters γ^{α}

In order to work with the update formulas (59)–(61) the incremental slip parameters γ^{α} must be determined. In this section we describe two approaches: the first approach (called *direct* method) is aimed to satisfy the conditions $\hat{\Phi}^{\alpha} = 0$ in conjunction with the incremental *Karush-Kuhn-Tucker* conditions in the form of Eqs. $(56)_1$–$(56)_3$, where $\alpha \in \mathscr{A}$ is associated with the *active* slip systems. This approach requires the search of an active set $\mathscr{A}$ and is aimed to satisfy *equalities* as well as *inequalities*. The second approach (called *indirect* method) focuses on the satisfaction of *equalities*, $\Theta^{\alpha} = 0$ say, which are equivalent to the Eqs. $(56)_1$–$(56)_3$ (equalities and inequalities). This approach is associated with *all* (active and inactive) slip systems, $\alpha = 1, \ldots, n$, (see [6] and [46]). The nonlinear functions Θ^{α} are defined so that the roots of $\Theta^{\alpha} = 0$ satisfy the incremental *Karush-Kuhn-Tucker* conditions *a priori*. Hence, the indirect method omits an active set search, which is a fundamental advantage when compared with the direct method.

(i) Direct method to determine γ^{α}. By estimating $\mathscr{A}$ and initializing the incremental slip parameters, $\gamma^{\alpha} \Leftarrow 0$, we employ an iterative procedure (local Newton iteration) to solve the nonlinear equations $\hat{\Phi}^{\alpha} = 0$, $\alpha \in \mathscr{A}$, with respect to γ^{α}. During the Newton iteration $\mathscr{A}$ is kept fixed and we may write for the update formulas

$$\begin{aligned}\gamma^{\alpha} &\Leftarrow \gamma^{\alpha} - \sum_{\beta \in \mathscr{A}} G^{\alpha\beta-1} \hat{\Phi}^{\beta}, \\ G^{\alpha\beta} &= \frac{\partial \hat{\Phi}^{\alpha}}{\partial \gamma^{\beta}} \quad \text{for} \quad \alpha, \beta \in \mathscr{A} \ ,\end{aligned} \tag{62}$$

where the coefficients $G^{\alpha\beta-1}$ form the entries of the matrices $[G^{\alpha\beta-1}]$, i.e. the inverse of the matrices $[G^{\alpha\beta}]$. In order to derive $G^{\alpha\beta}$ we apply Eqs. (31), (51), (59), and the chain rule. Thus, by means of Eqs. (37)–(39), $G^{\alpha\beta}$ follow from $(62)_2$ as

$$\begin{aligned}G^{\alpha\beta} = \mu &\left(2\mathbf{a}^{\alpha} \cdot \frac{\partial \mathbf{a}^{\alpha}}{\partial \gamma^{\beta}} - \frac{2}{3} \sum_{i=1}^{3} \mathbf{e}^{i} \cdot \frac{\partial \mathbf{e}^{i}}{\partial \gamma^{\beta}} \right) \\ &+ \sum_{\nu \in \mathscr{B}} \left\{ 4\psi^{\nu\nu} \mathbf{a}^{\nu} \cdot \frac{\partial \mathbf{a}^{\nu}}{\partial \gamma^{\beta}} \left(A^{\nu\alpha} a^{\alpha\nu} - \frac{1}{3} \bar{I}_4^{\nu} \right) \right. \\ &\left. + 2\psi^{\nu} \left[A^{\nu\alpha} \left(\mathbf{a}^{\alpha} \cdot \frac{\partial \mathbf{a}^{\nu}}{\partial \gamma^{\beta}} + \frac{\partial \mathbf{a}^{\alpha}}{\partial \gamma^{\beta}} \cdot \mathbf{a}^{\nu} \right) - \frac{2}{3} \mathbf{a}^{\nu} \cdot \frac{\partial \mathbf{a}^{\nu}}{\partial \gamma^{\beta}} \right] \right\} \\ &- \frac{\partial B}{\partial A} \ ,\end{aligned} \tag{63}$$

where we have introduced the elasticity functions

$$\psi^{\nu\nu} = \frac{\mathrm{d}^2 \bar{\Psi}_{\mathrm{f}}^{\nu}}{\mathrm{d}\bar{I}_4^{\nu} \mathrm{d}\bar{I}_4^{\nu}}, \quad \nu \in \mathscr{B} \ . \tag{64}$$

With the help of Eqs. $(60)_1$, $(61)_1$, the partial derivatives of $\mathbf{a}^{\alpha}$ and $\mathbf{e}^i$ with respect to γ^{β} give the relations

$$\frac{\partial \mathbf{a}^{\alpha}}{\partial \gamma^{\beta}} = \frac{1}{3} \mathbf{a}^{\alpha\,\mathrm{tr}} - A^{\alpha\beta} \mathbf{a}^{\beta\,\mathrm{tr}}, \quad \frac{\partial \mathbf{e}^{i}}{\partial \gamma^{\beta}} = \frac{1}{3} \mathbf{e}^{i\,\mathrm{tr}} - B^{i\beta} \mathbf{a}^{\beta\,\mathrm{tr}} \ , \tag{65}$$

which are independent of the incremental slip parameters γ^{α}.

Using (35) we then obtain from (64)

$$\psi^{\nu\nu} = k_1 [1 + 2k_2 (\bar{I}_4^{\nu} - 1)^2] \exp[k_2 (\bar{I}_4^{\nu} - 1)^2] \ . \tag{66}$$

The disadvantage of this approach is that an estimation of the active set $\mathscr{A}$ is required, which, in general, has to be updated more or less on a trial and error basis, see Box 2(d).

Remark 3.1. In this remark we point out a (known) numerical problem of the direct method associated with multisurface plasticity. The problem arises from the nonsmooth yield surface $\partial\mathbb{E}$. A possible numerical treatment is discussed.

An elastic trial step predicts a trial set $\{\alpha \in 1, \ldots, n | \hat{\Phi}^{\alpha} > 0\}$ of active slip systems (see Box 2(c)). Note that such predicted values $\hat{\Phi}^{\alpha} > 0$ do not, in general, imply that the associated incremental slip parameters γ^{α} are positive, since this is just a trial step [50]. In fact, several parameters γ^{α} could be negative, which is not consistent with the incremental *Karush-Kuhn-Tucker* conditions and the incremental consistency conditions (56). In addition, another fundamental difficulty of this approach is that several yield criterion functions predicted to be non-active could in fact be active at the solution point.

In order to handle this type of problem we redefine the active working set $\mathscr{A}$ (for more details see Box 2(d),

see also [32]), and introduce the set $\mathscr{A}^\gamma = \{\alpha \in 1,\dots,n | \gamma^\alpha > 0\}$ of positive incremental slip parameters and the set $\mathscr{A}^\Phi = \{\alpha \in 1,\dots,n | \hat{\Phi}^\alpha > \text{tol}\}$ of violated yield criteria, where $\text{tol} \in \mathbb{R}_+$ is a small (machine-dependent) tolerance value. The redefined working set is then the union $\mathscr{A} = \mathscr{A}^\gamma \cup \mathscr{A}^\Phi$. The interested reader is referred to [51], where this type of problem has been investigated in detail. □

Remark 3.2. If we consider the simplest case of one slip system ($n = 1$), relation (63) reduces to the form

$$G^{11} = -\frac{2}{3}\mu\left[2\mathbf{a}^1 \cdot \mathbf{a}^{1\,\mathrm{tr}} + \sum_{i=1}^{3}\left(\frac{1}{3}\mathbf{e}^i \cdot \mathbf{e}^{i\,\mathrm{tr}} - B^{1i}\mathbf{e}^i \cdot \mathbf{a}^{1\,\mathrm{tr}}\right)\right] - \frac{16}{9}\left(\psi^{11}a^{11} + \psi^1\right)\mathbf{a}^1 \cdot \mathbf{a}^{1\,\mathrm{tr}} - \frac{\partial B}{\partial A} \quad . \quad \square \tag{67}$$

Remark 3.3. For the computation of the coefficients $G^{\alpha\beta}$ through Eqs. (63) and (65) (or for one slip system through Eq. (67)), we suggest a numerical approximation of expression $(62)_2$ of the form [33]

$$G^{\alpha\beta} \approx \frac{1}{\delta}\left[\hat{\mathbf{\Phi}}^\alpha(\gamma^\beta + \delta) - \hat{\mathbf{\Phi}}^\alpha(\gamma^\beta)\right] \quad , \tag{68}$$

where δ is a small (machine-dependent) tolerance value.

From the practical point of view another simplification can be achieved by neglecting the neo-Hookean part, i.e. the first term in Eq. (63) (or Eq. (67)). This simplification is often appropriate for deformation states which are associated with plastic flow ($\mu \ll \psi^\alpha$, $\alpha \in \mathscr{B}$), in particular, for soft biological materials. This is in agreement with the histology of biological tissues since it is known that the (non-collageneous) matrix material, modeled by the neo-Hookean material, is dominant in the small strain domain, while the collagen-fibers, modeled by the exponential function, are the main load carrying components in the large strain domain in which the influence of the matrix material becomes negligible.

The suggested simplification does not influence significantly the quadratic rate of convergence near the solution point when Newton's method is applied. □

(ii) Indirect method to determine γ^α. Equivalent equalities to the equalities *and* inequalities $(56)_1$–$(56)_3$ turn out to be of the form

$$\Theta^\alpha = \sqrt{(\hat{\Phi}^\alpha)^2 + (\gamma^\alpha)^2} + \hat{\Phi}^\alpha - \gamma^\alpha = 0 \quad . \tag{69}$$

By employing an iterative procedure (local Newton iteration) in order to solve Eq. $(69)_2$ we may compute the incremental slip parameters γ^α, *and*, consequently, the set of active slip systems $\mathscr{A}$ is determined, see Box 2(e). The associated update formulas read

$$\begin{aligned} \gamma^\alpha &\Leftarrow \gamma^\alpha - \sum_{\beta=1}^{n} H^{\alpha\beta-1}\Theta^\beta, \\ H^{\alpha\beta} &= \frac{\partial \Theta^\alpha}{\partial \gamma^\beta} \ \text{ for } \ \alpha,\beta = 1,\dots,n \ . \end{aligned} \tag{70}$$

In order to determine the $n \times n$ matrix $H^{\alpha\beta}$ we differentiate Eq. $(69)_1$ with respect to γ^α and use definition Eq. $(62)_2$. Hence, we obtain a relation between $H^{\alpha\beta}$ and $G^{\alpha\beta}$ according to

$$H^{\alpha\beta} = (c^\alpha \hat{\mathbf{\Phi}}^\alpha + 1)G^{\alpha\beta} + (c^\alpha\gamma^\alpha - 1)\delta_{\alpha\beta} \ \ (\text{no summation over } \alpha) \ , \tag{71}$$

where $G^{\alpha\beta}$ is defined in Eq. (63) and the scalar functions c^α are the abbreviations for $[(\hat{\mathbf{\Phi}}^\alpha)^2 + (\gamma^\alpha)^2]^{-1/2}$. Note that in Eq. (71) the matrix $G^{\alpha\beta}$ has to be computed for all (active and inactive) slip systems, i.e. $\alpha,\beta = 1,\dots,n$. Hence, the more slip systems considered the higher are the computational costs to compute the inverse of the $n \times n$ matrix $H^{\alpha\beta}$. The main advantage of the indirect method, which only involves equations, is, that the plastic corrector procedure works without estimating the set $\mathscr{A}$ of active slip systems.

For the case of linearly dependent (or redundant) constraints, which are the yield criterion functions on the different slip systems, the matrix $[G^{\alpha\beta}]$ (or $[H^{\alpha\beta}]$) is singular and not invertible, as it is needed in Eq. (62) (or Eq. (70)). Hence, the incremental slip parameter γ^α on the active slip system is not *uniquely* defined. Note that, this is, for example, the case if $|\mathbf{a}_0^\alpha \cdot \mathbf{a}_0^\beta| = 1$ for $\alpha \neq \beta$. For a solution procedure to circumvent the problem of linearly dependent constraints the reader is referred to, for example, Miehe [32] or Miehe and Schröder [34].

4 Elastoplastic moduli

The aim now is to use the nonlinear stress relations postulated in Sect. 2 within a finite element formulation. The application of incremental/iterative solution techniques requires a consistent linearization of the nonlinear function $\boldsymbol{\tau}$ in order to preserve quadratic rate of convergence near the solution point. Hence, we have to derive the elastoplastic moduli $\mathbb{c}$, defined as

$$\mathbb{c} = 2\frac{\partial \boldsymbol{\tau}}{\partial \mathbf{g}} \quad . \tag{72}$$

Using the representation (41) of the Kirchhoff stress tensor $\boldsymbol{\tau}$, the elastoplastic moduli may be given in the decoupled form

$$\mathbb{c} = \mathbb{c}_{\mathrm{L}} + \bar{\mathbb{c}}, \quad \bar{\mathbb{c}} = \bar{\mathbb{c}}^{\mathrm{e}}_{\mathrm{gs}} + \bar{\mathbb{c}}^{\mathrm{e}}_{\mathrm{f}} + \bar{\mathbb{c}}^{\mathrm{p}}_{\mathrm{gs}} + \bar{\mathbb{c}}^{\mathrm{p}}_{\mathrm{f}} \quad . \tag{73}$$

The three elastic moduli $\mathbb{c}_{\mathrm{L}}$, $\bar{\mathbb{c}}^{\mathrm{e}}_{\mathrm{gs}}$, $\bar{\mathbb{c}}^{\mathrm{e}}_{\mathrm{f}}$ follow from Eqs. (47) and are governed by the relations

$$\mathbb{c}_{\mathrm{L}} = 2\frac{\partial \boldsymbol{\tau}_{\mathrm{L}}}{\partial \mathbf{g}} = J\left(p + J\frac{\mathrm{d}p}{\mathrm{d}J}\right)\mathbf{I}\otimes\mathbf{I} - 2Jp\,\mathbb{I} \quad , \tag{74}$$

$$\bar{\mathbb{c}}^{\mathrm{e}}_{\mathrm{gs}} = 2\frac{\partial \tilde{\boldsymbol{\tau}}_{\mathrm{gs}}}{\partial \mathbf{g}}\bigg|_{\gamma^\alpha} = \frac{2}{3}\mu\,\mathrm{tr}\bar{\mathbf{b}}^{\mathrm{e}}\left(\mathbb{I} - \frac{1}{3}\mathbf{I}\otimes\mathbf{I}\right) - \frac{2}{3}\left(\tilde{\boldsymbol{\tau}}_{\mathrm{gs}}\otimes\mathbf{I} + \mathbf{I}\otimes\tilde{\boldsymbol{\tau}}_{\mathrm{gs}}\right) \quad , \tag{75}$$

$$\bar{\mathbb{c}}_{\mathrm{f}}^{\mathrm{e}} = 2\sum_{\alpha\in\mathscr{B}} \left.\frac{\partial\tilde{\boldsymbol{\tau}}_{\mathrm{f}}^{\alpha}}{\partial\mathbf{g}}\right|_{\gamma^{\alpha}} = 4\sum_{\alpha\in\mathscr{B}}\Big\{\frac{1}{3}\psi^{\alpha}[\bar{I}_4^{\alpha}(\mathbb{I}+\frac{1}{3}\mathbf{I}\otimes\mathbf{I}) - (\mathbf{a}^{\alpha}\otimes\mathbf{a}^{\alpha})\otimes\mathbf{I} - \mathbf{I}\otimes(\mathbf{a}^{\alpha}\otimes\mathbf{a}^{\alpha})] + \psi^{\alpha\alpha}\,\mathrm{dev}(\mathbf{a}^{\alpha}\otimes\mathbf{a}^{\alpha})\otimes\mathrm{dev}(\mathbf{a}^{\alpha}\otimes\mathbf{a}^{\alpha})\Big\}, \tag{76}$$

where the specifications for the hydrostatic pressure p, the stress functions ψ^{α} and the elasticity functions $\psi^{\alpha\alpha}$ are given in (49) and (66). The closed-form expressions for the elastic moduli $\mathbb{c}_{\mathrm{L}}$ and $\bar{\mathbb{c}}_{\mathrm{gs}}^{\mathrm{e}}$ are known from finite elasticity [31]. The expression $\bar{\mathbb{c}}_{\mathrm{f}}^{\mathrm{e}}$ for the elastic anisotropic contribution is derived in Appendix A.2.

The plastic parts of $\mathbb{c}$ are defined as

$$\bar{\mathbb{c}}_{\mathrm{gs}}^{\mathrm{p}} = 2\sum_{\alpha\in\mathscr{A}}\frac{\partial\tilde{\boldsymbol{\tau}}_{\mathrm{gs}}}{\partial\gamma^{\alpha}}\otimes\frac{\partial\gamma^{\alpha}}{\partial\mathbf{g}}, \quad \bar{\mathbb{c}}_{\mathrm{f}}^{\mathrm{p}} = 2\sum_{\beta\in\mathscr{B}}\sum_{\alpha\in\mathscr{A}}\frac{\partial\tilde{\boldsymbol{\tau}}_{\mathrm{f}}^{\beta}}{\partial\gamma^{\alpha}}\otimes\frac{\partial\gamma^{\alpha}}{\partial\mathbf{g}} \quad . \tag{77}$$

In order to calculate the derivatives with respect to γ^{α}, we need the algorithmic expression of $\bar{\mathbf{b}}^{\mathrm{e}}$. With the help of Eqs. (57) and $(58)_2$, we find from (5) that

$$\bar{\mathbf{b}}^{\mathrm{e}} = \bar{\mathbf{b}}^{\mathrm{e\,tr}} - 2\sum_{\alpha\in\mathscr{A}}\gamma^{\alpha}\Big(\mathbf{a}^{\alpha\,\mathrm{tr}}\otimes\mathbf{a}^{\alpha\,\mathrm{tr}} - \tfrac{1}{3}\bar{\mathbf{b}}^{\mathrm{e\,tr}}\Big) + \sum_{\alpha\in\mathscr{A}}\sum_{\beta\in\mathscr{A}}\gamma^{\alpha}\gamma^{\beta}\big(A^{\alpha\beta}\mathbf{a}^{\alpha\,\mathrm{tr}}\otimes\mathbf{a}^{\beta\,\mathrm{tr}} - \tfrac{1}{3}\mathbf{a}^{\alpha\,\mathrm{tr}}\otimes\mathbf{a}^{\alpha\,\mathrm{tr}} - \tfrac{1}{3}\mathbf{a}^{\beta\,\mathrm{tr}}\otimes\mathbf{a}^{\beta\,\mathrm{tr}} + \tfrac{1}{9}\bar{\mathbf{b}}^{\mathrm{e\,tr}}\big) \quad , \tag{78}$$

where the definition $\bar{\mathbf{b}}^{\mathrm{e\,tr}} = \bar{\mathbf{F}}^{\mathrm{e\,tr}}(\bar{\mathbf{F}}^{\mathrm{e\,tr}})^{\mathrm{T}}$ has been introduced.

Based on (78) and some straightforward manipulations (see Appendix B.1), we obtain the derivative of the isotropic contribution to the stress with respect to the incremental slip parameters γ^{α}, i.e.

$$\frac{\partial\tilde{\boldsymbol{\tau}}_{\mathrm{gs}}}{\partial\gamma^{\alpha}} = -\mu\,\mathrm{dev}\Big[2\Big(\mathbf{a}^{\alpha\,\mathrm{tr}}\otimes\mathbf{a}^{\alpha\,\mathrm{tr}} - \frac{1}{3}\bar{\mathbf{b}}^{\mathrm{e\,tr}}\Big) - 2\sum_{\beta\in\mathscr{A}}\gamma^{\beta}\Big(A^{\alpha\beta}\mathbf{a}^{\alpha\,\mathrm{tr}}\otimes\mathbf{a}^{\beta\,\mathrm{tr}} - \frac{1}{3}\mathbf{a}^{\alpha\,\mathrm{tr}}\otimes\mathbf{a}^{\alpha\,\mathrm{tr}} - \frac{1}{3}\mathbf{a}^{\beta\,\mathrm{tr}}\otimes\mathbf{a}^{\beta\,\mathrm{tr}} + \frac{1}{9}\bar{\mathbf{b}}^{\mathrm{e\,tr}}\Big)\Big] \quad . \tag{79}$$

By applying the implicit function theorem to (31), the derivative of the parameters γ^{α} with respect to the Eulerian metric $\mathbf{g}$ yields

$$\frac{\partial\gamma^{\alpha}}{\partial\mathbf{g}} = \sum_{\beta\in\mathscr{A}} G^{\alpha\beta-1}\frac{\partial\hat{\boldsymbol{\Phi}}^{\beta}}{\partial\mathbf{g}} \quad , \tag{80}$$

where the coefficients $G^{\alpha\beta-1}$ form the entries of the matrices $[G^{\alpha\beta-1}]$ (compare with Eq. (63)). Applying the chain rule to Eq. (51) we find, after some algebra (see Appendix B.2), that

$$\frac{\partial\hat{\boldsymbol{\Phi}}^{\beta}}{\partial\mathbf{g}} = \mu\;\mathrm{dev}\Big(\mathbf{a}^{\beta}\otimes\mathbf{a}^{\beta} - \frac{1}{3}\bar{\mathbf{b}}^{\mathrm{e}}\Big) + 2\,\mathrm{dev}\sum_{\nu\in\mathscr{B}}\Big\{\psi^{\nu\nu}\Big(A^{\beta\nu}a^{\beta\nu} - \frac{1}{3}a^{\nu\nu}\Big)(\mathbf{a}^{\nu}\otimes\mathbf{a}^{\nu}) + \psi^{\nu}\Big[\frac{1}{2}A^{\beta\nu}\big(\mathbf{a}^{\beta}\otimes\mathbf{a}^{\nu} + \mathbf{a}^{\nu}\otimes\mathbf{a}^{\beta}\big) - \frac{1}{3}\mathbf{a}^{\nu}\otimes\mathbf{a}^{\nu}\Big]\Big\} \quad . \tag{81}$$

By the use of Eq. $(47)_3$, the definitions of the invariants $\bar{I}_4^{\alpha} = \mathbf{a}^{\alpha}\cdot\mathbf{a}^{\alpha}$ and the chain and product rules, the derivative of the anisotropic contribution of the stress with respect to the incremental slip parameters, as required in Eq. $(77)_2$, may be written as

$$\frac{\partial\tilde{\boldsymbol{\tau}}_{\mathrm{f}}^{\beta}}{\partial\gamma^{\alpha}} = 4\psi^{\beta\beta}\Big(\mathbf{a}^{\beta}\cdot\frac{\partial\mathbf{a}^{\beta}}{\partial\gamma^{\alpha}}\Big)\mathrm{dev}\big(\mathbf{a}^{\beta}\otimes\mathbf{a}^{\beta}\big) + 2\psi^{\beta}\mathrm{dev}\Big(\mathbf{a}^{\beta}\otimes\frac{\partial\mathbf{a}^{\beta}}{\partial\gamma^{\alpha}} + \frac{\partial\mathbf{a}^{\beta}}{\partial\gamma^{\alpha}}\otimes\mathbf{a}^{\beta}\Big) \quad , \tag{82}$$

where the derivatives of the Eulerian vectors $\mathbf{a}^{\beta}$ with respect to the incremental slip parameters γ^{α} are defined via $(65)_1$.

Remark 4.1. If we consider the simplest case of one slip system ($n = 1$), the contributions to the elastoplastic moduli $\bar{\mathbb{c}}_{\mathrm{gs}}$ take on the reduced forms

$$\bar{\mathbb{c}}_{\mathrm{gs}}^{\mathrm{p}} = 2\frac{\partial\tilde{\boldsymbol{\tau}}_{\mathrm{gs}}}{\partial\gamma^{1}}\otimes\frac{\partial\gamma^{1}}{\partial\mathbf{g}}, \bar{\mathbb{c}}_{\mathrm{f}}^{\mathrm{p}} = 2\frac{\partial\tilde{\boldsymbol{\tau}}_{\mathrm{f}}^{1}}{\partial\gamma^{1}}\otimes\frac{\partial\gamma^{1}}{\partial\mathbf{g}} \quad , \tag{83}$$

with the expressions

$$\frac{\partial\tilde{\boldsymbol{\tau}}_{\mathrm{gs}}}{\partial\gamma^{1}} = -\mu\,\mathrm{dev}\Big[2\Big(1-\frac{1}{3}\gamma^{1}\Big)\big(\mathbf{a}^{1\,\mathrm{tr}}\otimes\mathbf{a}^{1\,\mathrm{tr}}\big) - \frac{2}{3}\Big(1+\frac{1}{3}\gamma^{1}\Big)\bar{\mathbf{b}}^{\mathrm{e\,tr}}\Big], \tag{84}$$

$$\frac{\partial\gamma^{1}}{\partial\mathbf{g}} = G^{11-1}\mathrm{dev}\Big[\mu\Big(\mathbf{a}^{1}\otimes\mathbf{a}^{1} - \frac{1}{3}\bar{\mathbf{b}}^{\mathrm{e}}\Big) + \frac{4}{3}\big(2\psi^{11}a^{11} + \psi^{1}\big)\big(\mathbf{a}^{1}\otimes\mathbf{a}^{1}\big)\Big], \tag{85}$$

$$\frac{\partial\tilde{\boldsymbol{\tau}}_{\mathrm{f}}^{1}}{\partial\gamma^{1}} = -\frac{4}{3}\mathrm{dev}\big[2\psi^{11}\big(\mathbf{a}^{1}\cdot\mathbf{a}^{1\,\mathrm{tr}}\big)\big(\mathbf{a}^{1}\otimes\mathbf{a}^{1}\big) + \psi^{1}\big(\mathbf{a}^{1}\otimes\mathbf{a}^{1\,\mathrm{tr}} + \mathbf{a}^{1\,\mathrm{tr}}\otimes\mathbf{a}^{1}\big)\big] \quad , \tag{86}$$

which are associated with relations (79), (80) and (82). □

Finally, the Eulerian elastoplastic modulus $\mathbb{c}$ is determined by summation of the three elastic contributions, given by Eqs. (74), (75) and (76), and the two plastic counterparts, given by Eqs. $(77)_1$ and $(77)_2$.

The flow chart as shown in Fig. 3 outlines the numerical implementation procedure of the material model. The different steps of the computation are summarized in Box 2(a)–(g), which contains all the relevant expressions necessary to compute the isochoric stress tensor $\tilde{\boldsymbol{\tau}}$ and the associated isochoric elastoplastic moduli $\bar{\mathbb{c}}$.

5 Representative numerical examples

The material model has been implemented in Version 7.3 of the multi-purpose finite element analysis program FEAP, originally developed by R.L. Taylor and documented in [58]. We have used 8-node $Q1/P0$ and $QM1/E12$ mixed finite elements. Both element descriptions are based on three-field Hu-Washizu variational formulations, which were proposed by Simo [53], [49], and successfully used by, for example, Miehe [32], Weiss et al. [59] and Holzapfel et al. [20], among many others.

The representative numerical examples aim to demonstrate the basic features and the good numerical

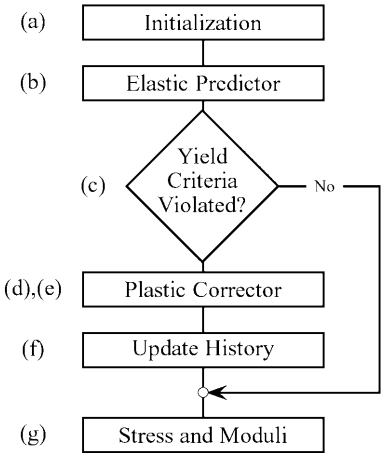

Fig. 3. Flow chart showing the different steps for a numerical implementation of the material model. Steps (a)–(g) of the computation are outlined in detail in Box 2(a)–(g). Steps (d) and (e) are alternatives and associated with the direct and indirect methods

performance of the material model implemented. We present two examples, whereby the first one aims to demonstrate basic elastic and inelastic mechanisms by means of a single cube which is reinforced by one fiber family. The second example demonstrates a three-dimensional necking phenomena by means of a rectangular bar under tension.

5.1 Anisotropic finite inelastic deformation of a single brick element

This example investigates the proposed constitutive framework by means of a simple and illustrative model problem. We consider a cube of length 1.0 cm which is reinforced by one family of fibers, as illustrated in Fig. 4. The orientation of the fiber reinforcement and the slip system (which is assumed to be one ($n = 1$)) is given by the unit direction vector $\mathbf{a}_0$. The cube is modeled by one 8-node isoparametric brick element based on a $Q1/P0$ mixed finite element formulation with an augmented Lagrangian extension. This choice avoids 'volumetric locking' phenomena so that incompressibility constraints can be incorporated without the disadvantage of an ill-conditioned global (tangent) stiffness matrix [53].

The boundary conditions are chosen in such a way that node 1 is fixed in all three directions ($\hat{u}_{11} = \hat{u}_{12} = \hat{u}_{13} = 0$), node 2 in the second and third direction ($\hat{u}_{21} = \hat{u}_{23} = 0$) while nodes 3 and 4 are fixed in the third direction ($\hat{u}_{33} = 0$) and ($\hat{u}_{43} = 0$). We deform the cube by prescribing the displacements in the third direction at the nodes 5, 6, 7 and 8 ($\hat{u}_{53} = \hat{u}_{63} = \hat{u}_{73} = \hat{u}_{83} = u$). The material parameters used for the calculation are collected in Table 1.

One result of this calculation is shown in Fig. 5, in which the reaction force F (summation over the nodal forces of nodes 5, 6, 7 and 8) is plotted against the displacement u. Significant states of deformation are labeled, starting with Ⓐ, which denotes the (undeformed) reference configuration of the cube. The next state of interest is Ⓑ, where the stress state touches the initial yield surface and plastic slipping takes place for the first time (the associated reaction force F is 15.31 (N) and the displacement u is 0.64 cm). During continuous loading the reaction force F increases and reaches its maximum $F = 26.44$ (N) at the displacement $u = 1.071$ cm, i.e. state Ⓒ. By increasing the displacement up to $u = 2.0$ cm (maximum displacement), i.e. state Ⓓ, the reaction force F takes on the value

Box 2(a)–(c). Implementation guide: initialization (a), elastic predictor (b) and check of the yield criteria (c)

(a) Initialization
History variables $\mathbf{F}_n^{p-1}$, A_n at time t_n
Deformation gradient $\mathbf{F}$ at actual time t_{n+1}
Slip systems $\mathbf{a}_0^\alpha$, $\alpha = 1, \ldots, n$

(b) Elastic Predictor

Jacobian determinant	$J = \det \mathbf{F}$
Unimodular part of the elastic deformation gradient	$\boxed{\overline{\mathbf{F}}^e = J^{-1/3}\mathbf{F}\mathbf{F}_n^{p-1}}$
Hardening variable	$\boxed{A = A_n}$

(c) Yield Criteria Check

Structural measures	$A^{\alpha\beta} = \mathbf{a}_0^\alpha \cdot \mathbf{a}_0^\beta, \quad \alpha, \beta = 1, \ldots, n$
Eulerian vectors	$\mathbf{a}^\alpha = \overline{\mathbf{F}}^e \mathbf{a}_0^\alpha, \quad \alpha = 1, \ldots, n$ $\mathbf{e}^i = \overline{\mathbf{F}}^e \mathbf{e}_0^i, \quad i = 1, 2, 3$
Deformed structural measures	$a^{\alpha\beta} = \mathbf{a}^\alpha \cdot \mathbf{a}^\beta, \quad \alpha, \beta = 1, \ldots, n$
Set of stretched fibers	$\mathscr{B} = \{\alpha \in 1, \ldots, n \mid a^{\alpha\alpha} > 1\}$
Stress functions	$\psi^\alpha = k_1(a^{\alpha\alpha} - 1)\exp[k_2(a^{\alpha\alpha} - 1)^2], \quad \alpha \in \mathscr{B}$
Micro-stress function	$\Phi_{\text{micro}} = \tau_0 + B, \quad B = hA + \tau_{0,\infty}[1 - \exp(-A/a_0)]$
Macro-stress functions	$\tau^\alpha = \mu(a^{\alpha\alpha} - \frac{1}{3}\sum_{i=1}^{3} \mathbf{e}^i \cdot \mathbf{e}^i) + 2 \sum_{\beta \in \mathscr{B}} \psi^\beta (A^{\alpha\beta} a^{\alpha\beta} - \frac{1}{3} a^{\beta\beta}), \quad \alpha = 1, \ldots, n$
Yield criterion functions	$\boxed{\hat{\Phi}^\alpha = \tau^\alpha - \Phi_{\text{micro}}, \quad \alpha = 1, \ldots, n}$
Define active working set	$\mathscr{A} = \{\alpha \in 1, \ldots, n \mid \hat{\Phi}^\alpha > \text{tol}\}$

If $\mathscr{A} = \emptyset$ compute modified elastic left Cauchy-Green tensor $\overline{\mathbf{b}}^e = \overline{\mathbf{F}}^e \overline{\mathbf{F}}^{eT}$ and goto Box 2(g).

Box 2(d). Implementation guide: plastic corrector – *direct method*

(d) Plastic Corrector – *direct method*

Initialize
$$\overline{\mathbf{F}}^{\mathrm{e}\,\mathrm{tr}} = \overline{\mathbf{F}}^{\mathrm{e}},\quad A^{\mathrm{tr}} = A,\quad \mathbf{a}^{\alpha\,\mathrm{tr}} = \mathbf{a}^{\alpha},\quad \mathbf{e}^{i\,\mathrm{tr}} = \mathbf{e}^{i},\quad \alpha = 1,\dots,n,\quad i = 1,2,3$$

Partial derivatives
$$\frac{\partial \mathbf{a}^{\alpha}}{\partial \gamma^{\beta}} = \frac{1}{3}\mathbf{a}^{\alpha\,\mathrm{tr}} - A^{\alpha\beta}\mathbf{a}^{\beta\,\mathrm{tr}},\quad \alpha,\beta = 1,\dots,n$$
$$\frac{\partial \mathbf{e}^{i}}{\partial \gamma^{\beta}} = \frac{1}{3}\mathbf{e}^{i\,\mathrm{tr}} - B^{i\beta}\mathbf{a}^{\beta\,\mathrm{tr}},\quad i = 1,2,3,\quad \beta = 1,\dots,n$$

→ Initialize
$$\gamma^{\alpha} = 0,\quad \alpha = 1,\dots,n$$

→ Deformed structural measures
$$a^{\alpha\beta} = \mathbf{a}^{\alpha}\cdot\mathbf{a}^{\beta},\quad \alpha,\beta \in \mathscr{A}\cup\mathscr{B}$$

Stress functions
$$\psi^{\alpha} = k_1(a^{\alpha\alpha}-1)\exp[k_2(a^{\alpha\alpha}-1)^2],\quad \alpha\in\mathscr{B}$$

Elasticity functions
$$\psi^{\alpha\alpha} = k_1[1+2k_2(a^{\alpha\alpha}-1)^2]\exp[k_2(a^{\alpha\alpha}-1)^2],\quad \alpha\in\mathscr{B}$$

Micro-stress function
$$\Phi_{\mathrm{micro}} = \tau_0 + B,\quad B = hA + \tau_{0,\infty}[1-\exp(-A/a_0)]$$

Macro-stress functions
$$\tau^{\alpha} = \mu\left(a^{\alpha\alpha} - \frac{1}{3}\sum_{i=1}^{3}\mathbf{e}^{i}\cdot\mathbf{e}^{i}\right) + 2\sum_{\beta\in\mathscr{B}}\psi^{\beta}\left(A^{\alpha\beta}a^{\alpha\beta} - \tfrac{1}{3}a^{\beta\beta}\right),\quad \alpha\in\mathscr{A}$$

Yield criterion functions
$$\hat{\mathbf{\Phi}}^{\alpha} = \tau^{\alpha} - \Phi_{\mathrm{micro}},\quad \alpha\in\mathscr{A}$$

Partial derivative
$$\frac{\partial B}{\partial A} = h + \frac{\tau_{0,\infty}}{a_0}\exp(-A/a_0)$$

$$G^{\alpha\beta} = \mu\left(2\mathbf{a}^{\alpha}\cdot\frac{\partial \mathbf{a}^{\alpha}}{\partial\gamma^{\beta}} - \frac{2}{3}\sum_{i=1}^{3}\mathbf{e}^{i}\cdot\frac{\partial\mathbf{e}^{i}}{\partial\gamma^{\beta}}\right) + \sum_{\nu\in\mathscr{B}}\left\{4\psi^{\nu\nu}\mathbf{a}^{\nu}\cdot\frac{\partial\mathbf{a}^{\nu}}{\partial\gamma^{\beta}}\left(A^{\alpha\nu}a^{\alpha\nu} - \frac{1}{3}a^{\nu\nu}\right)\right.$$
$$\left. + 2\psi^{\nu}\left[A^{\alpha\nu}\left(\mathbf{a}^{\alpha}\cdot\frac{\partial\mathbf{a}^{\nu}}{\partial\gamma^{\beta}} + \frac{\partial\mathbf{a}^{\alpha}}{\partial\gamma^{\beta}}\cdot\mathbf{a}^{\nu}\right) - \frac{2}{3}\mathbf{a}^{\nu}\cdot\frac{\partial\mathbf{a}^{\nu}}{\partial\gamma^{\beta}}\right]\right\} - \frac{\partial B}{\partial A},\quad \alpha,\beta\in\mathscr{A}$$

Update
$$\gamma^{\alpha} \Leftarrow \gamma^{\alpha} - \sum_{\beta\in\mathscr{A}} G^{\alpha\beta-1}\hat{\mathbf{\Phi}}^{\beta},\quad \alpha\in\mathscr{A}$$
$$A \Leftarrow A^{\mathrm{tr}} + \sum_{\alpha\in\mathscr{A}}\gamma^{\alpha}$$
$$\mathbf{a}^{\alpha} \Leftarrow \mathbf{a}^{\alpha\,\mathrm{tr}} - \sum_{\beta\in\mathscr{A}}\gamma^{\beta}\left(\mathbf{a}^{\beta\,\mathrm{tr}}A^{\alpha\beta} - \frac{1}{3}\mathbf{a}^{\alpha\,\mathrm{tr}}\right),\quad \alpha\in\mathscr{A}\cup\mathscr{B}$$
$$\mathbf{e}^{i} \Leftarrow \mathbf{e}^{i\,\mathrm{tr}} - \sum_{\beta\in\mathscr{A}}\gamma^{\beta}\left(\mathbf{a}^{\beta\,\mathrm{tr}}B^{i\beta} - \frac{1}{3}\mathbf{e}^{i\,\mathrm{tr}}\right),\quad i = 1,2,3$$

Redefine set of stretched fibers $\mathscr{B} = \{\alpha\in 1,\dots,n | a^{\alpha\alpha} > 1\}$

DO UNTIL $\hat{\mathbf{\Phi}}^{\alpha} < \mathrm{tol},\quad \alpha\in\mathscr{A}$

Set up $\mathscr{A}^{\gamma} = \{\alpha\in 1,\dots,n|\gamma^{\alpha} > 0\}$ and $\mathscr{A}^{\Phi} = \{\alpha\in 1,\dots,n|\hat{\mathbf{\Phi}}^{\alpha} > \mathrm{tol}\}$
Redefine active working set $\mathscr{A} \Leftarrow \mathscr{A}^{\gamma}\cup\mathscr{A}^{\Phi}$

DO UNTIL $\gamma^{\alpha} \geq 0$ AND $\hat{\mathbf{\Phi}}^{\alpha} < \mathrm{tol},\quad \alpha = 1,\dots,n$

Update modified elastic deformation gradient
$$\overline{\mathbf{F}}^{\mathrm{e}} \Leftarrow \overline{\mathbf{F}}^{\mathrm{e}\,\mathrm{tr}} - \sum_{\alpha\in\mathscr{A}}\gamma^{\alpha}\left(\mathbf{a}^{\alpha\,\mathrm{tr}}\otimes\mathbf{a}_0^{\alpha} - \frac{1}{3}\overline{\mathbf{F}}^{\mathrm{e}\,\mathrm{tr}}\right)$$

22.82 (N). Note that from state Ⓑ on, plastic strains increase continuously up to state Ⓓ. Now we unload ($F = 0.0$ (N)) and reach state Ⓔ with the residual displacement $u = 0.206$ cm. The associated stress-free configuration of the cube can be seen in Fig. 6, which differs significantly from the (undeformed) reference configuration. A continuous reduction of the displacement to $u = 0$ leads to state Ⓕ which is accompanied by compressive stress ($F = -1.4$ (N)).

Note that the large hysteresis in Fig. 5 clearly indicates the plastic dissipation of the proposed material model. In addition, the plot displays pronounced softening which occurs due to the highly nonlinear deformations. It is clearly a geometrical effect since the component of the Cauchy stress in $\mathbf{e}_3$-direction, i.e. σ_{33}, monotonically increases with respect to the displacement u during loading, see Fig. 7.

The spatial configurations of the cube at different load states are illustrated in Fig. 6. Interestingly enough, the elastic part of the deformation moves the top face of the cube to the left, while the plastic part moves it to the right. This remarkable effect may be explained by the orientation of the fiber reinforcement (the slip system). During the elastic deformation the fibers tend to align with the

Box 2(e). Implementation guide: plastic corrector – *indirect method*, ($\alpha, \beta = 1, \ldots, n$ and $i = 1, 2, 3$)

(e) Plastic Corrector – *indirect method*

Initialize
$$\overline{\mathbf{F}}^{\mathrm{e}\,\mathrm{tr}} = \overline{\mathbf{F}}^{\mathrm{e}}, \quad A^{\mathrm{tr}} = A, \quad \mathbf{a}^{\alpha\,\mathrm{tr}} = \mathbf{a}^{\alpha}, \quad \mathbf{e}^{i\,\mathrm{tr}} = \mathbf{e}^{i}$$

Partial derivatives
$$\frac{\partial \mathbf{a}^{\alpha}}{\partial \gamma^{\beta}} = \frac{1}{3}\mathbf{a}^{\alpha\,\mathrm{tr}} - A^{\alpha\beta}\mathbf{a}^{\beta\,\mathrm{tr}}$$
$$\frac{\partial \mathbf{e}^{i}}{\partial \gamma^{\beta}} = \frac{1}{3}\mathbf{e}^{i\,\mathrm{tr}} - B^{i\beta}\mathbf{a}^{\beta\,\mathrm{tr}}$$

Initialize
$$\gamma^{\alpha} = 0$$

Deformed structural measures
$$a^{\alpha\beta} = \mathbf{a}^{\alpha} \cdot \mathbf{a}^{\beta}$$

Stress functions
$$\psi^{\alpha} = k_1(a^{\alpha\alpha} - 1)\exp[k_2(a^{\alpha\alpha} - 1)^2]$$

Elasticity functions
$$\psi^{\alpha\alpha} = k_1[1 + 2k_2(a^{\alpha\alpha} - 1)^2]\exp[k_2(a^{\alpha\alpha} - 1)^2]$$

Micro-stress function
$$\Phi_{\mathrm{micro}} = \tau_0 + B, \quad B = hA + \tau_{0,\infty}[1 - \exp(-A/a_0)]$$

Macro-stress functions
$$\tau^{\alpha} = \mu\left(a^{\alpha\alpha} - \tfrac{1}{3}\sum_{i=1}^{3}\mathbf{e}^{i}\cdot\mathbf{e}^{i}\right) + 2\sum_{\beta\in\mathscr{B}}\psi^{\beta}\left(A^{\alpha\beta}a^{\alpha\beta} - \tfrac{1}{3}a^{\beta\beta}\right)$$

Yield criterion functions
$$\hat{\mathbf{\Phi}}^{\alpha} = \tau^{\alpha} - \Phi_{\mathrm{micro}}$$

Equivalent equalities
$$\Theta^{\alpha} = \sqrt{(\hat{\mathbf{\Phi}}^{\alpha})^2 + (\gamma^{\alpha})^2} + \hat{\mathbf{\Phi}}^{\alpha} - \gamma^{\alpha}$$

Partial derivative
$$\frac{\partial B}{\partial A} = h + \frac{\tau_{0,\infty}}{a_0}\exp(-A/a_0)$$

Scalars
$$c^{\alpha} = [(\hat{\mathbf{\Phi}}^{\alpha})^2 + (\gamma^{\alpha})^2]^{-1/2}$$

$$G^{\alpha\beta} = \mu\left(2\mathbf{a}^{\alpha}\cdot\frac{\partial \mathbf{a}^{\alpha}}{\partial\gamma^{\beta}} - \frac{2}{3}\sum_{i=1}^{3}\mathbf{e}^{i}\cdot\frac{\partial \mathbf{e}^{i}}{\partial\gamma^{\beta}}\right) + \sum_{\nu\in\mathscr{B}}\left\{4\psi^{\nu\nu}\mathbf{a}^{\nu}\cdot\frac{\partial \mathbf{a}^{\nu}}{\partial\gamma^{\beta}}\left(A^{\alpha\nu}a^{\alpha\nu} - \frac{1}{3}a^{\nu\nu}\right)\right.$$
$$\left. + 2\psi^{\nu}\left[A^{\alpha\nu}\left(\mathbf{a}^{\alpha}\cdot\frac{\partial \mathbf{a}^{\nu}}{\partial\gamma^{\beta}} + \frac{\partial \mathbf{a}^{\alpha}}{\partial\gamma^{\beta}}\cdot\mathbf{a}^{\nu}\right) - \frac{2}{3}\mathbf{a}^{\nu}\cdot\frac{\partial \mathbf{a}^{\nu}}{\partial\gamma^{\beta}}\right]\right\} - \frac{\partial B}{\partial A}$$
$$H^{\alpha\beta} = (c^{\alpha}\hat{\mathbf{\Phi}}^{\alpha} + 1)G^{\alpha\beta} + (c^{\alpha}\gamma^{\alpha} - 1)\delta_{\alpha\beta}$$

Update
$$\gamma^{\alpha} \Leftarrow \gamma^{\alpha} - \sum_{\beta=1}^{n} H^{\alpha\beta-1}\Theta^{\beta}$$
$$A \Leftarrow A^{\mathrm{tr}} + \sum_{\beta=1}^{n}\gamma^{\alpha}$$
$$\mathbf{a}^{\alpha} \Leftarrow \mathbf{a}^{\alpha\,\mathrm{tr}} - \sum_{\beta=1}^{n}\gamma^{\beta}\left(\mathbf{a}^{\beta\,\mathrm{tr}}A^{\alpha\beta} - \frac{1}{3}\mathbf{a}^{\alpha\,\mathrm{tr}}\right)$$
$$\mathbf{e}^{i} \Leftarrow \mathbf{e}^{i\,\mathrm{tr}} - \sum_{\beta=1}^{n}\gamma^{\beta}\left(\mathbf{a}^{\beta\,\mathrm{tr}}B^{i\beta} - \frac{1}{3}\mathbf{e}^{i\,\mathrm{tr}}\right)$$

Redefine set of stretched fibers $\mathscr{B} = \{\alpha \in 1, \ldots, n | a^{\alpha\alpha} > 1\}$

DO UNTIL $\Theta^{\alpha} < \mathrm{tol}, \quad \alpha = 1, \ldots, n$

Determine active working set and update modified elastic deformation gradient

$$\mathscr{A} = \{\alpha \in 1, \ldots, n | \gamma^{\alpha} > \mathrm{tol}\} \qquad \overline{\mathbf{F}}^{\mathrm{e}} \Leftarrow \overline{\mathbf{F}}^{\mathrm{e}\,\mathrm{tr}} - \sum_{\alpha\in\mathscr{A}}\gamma^{\alpha}\left(\mathbf{a}^{\alpha\,\mathrm{tr}}\otimes\mathbf{a}_0^{\alpha} - \frac{1}{3}\overline{\mathbf{F}}^{\mathrm{e}\,\mathrm{tr}}\right)$$

direction of loading (move to the left) and the plastic deformation is determined by the flow rule (18), which forces the top face to move to the right. In order to investigate the accuracy of the solution we have used 10 and 200 load steps to achieve the displacement $u = 2.0$ cm. A comparison of the two solutions indicated that 10 load steps are (practically) enough to get satisfying accuracy. Hence, it is sufficient to work with the first-order accurate backward-Euler discretization.

In Table 2 the residual norm is reported, showing quadratic rate of convergence of the out-of-balance forces near the solution point. In particular, Table 2 refers to the residual norm which occurs during the load step from $u = 1.8$ cm to $u = 2.0$ cm. Table 3 reports the spatial coordinates of the eight nodes of the deformation state Ⓓ.

Finally, it is noted that the proposed constitutive model is able to replicate characteristic plastic effects, such as hysteresis and residual strains (and stresses). The implementation of the model as described above leads to a numerically robust and efficient tool suitable for large scale computation.

5.2 Three-dimensional necking phenomena

This example models the extension of a rectangular bar with cross-section $a \times b$ and length l, within the elasto-

Box 2(f), (g). Implementation guide: history update (f), isochoric Kirchhoff stress and elastoplastic moduli (g)

(f) Update History

Inverse plastic deformation gradient $\boxed{\mathbf{F}_n^{\mathrm{p}-1} \Leftarrow J^{1/3}\mathbf{F}^{-1}\overline{\mathbf{F}}^{\mathrm{e}}}$

Hardening variable $\boxed{A_n \Leftarrow A}$

(g) Isochoric Kirchhoff Stress and Elastoplastic Moduli

Isochoric Kirchhoff stress $\boxed{\tilde{\boldsymbol{\tau}} = \mu\,\mathrm{dev}\overline{\mathbf{b}}^{\mathrm{e}} + 2\sum_{\alpha\in\mathscr{B}}\psi^{\alpha}\mathrm{dev}(\mathbf{a}^{\alpha}\otimes\mathbf{a}^{\alpha})}$

Isochoric elastoplastic moduli $\boxed{\overline{\mathbb{C}} = \overline{\mathbb{C}}^{\mathrm{e}}_{\mathrm{gs}} + \overline{\mathbb{C}}^{\mathrm{e}}_{\mathrm{f}} + \overline{\mathbb{C}}^{\mathrm{p}}_{\mathrm{gs}} + \overline{\mathbb{C}}^{\mathrm{p}}_{\mathrm{f}}}$

Elastic contributions to the isochoric moduli $\overline{\mathbb{C}}$

$$\overline{\mathbb{C}}^{\mathrm{e}}_{\mathrm{gs}} = \frac{2}{3}\mu\mathrm{tr}\overline{\mathbf{b}}^{\mathrm{e}}\left(\mathbb{I} - \frac{1}{3}\mathbf{I}\otimes\mathbf{I}\right) - \frac{2}{3}\mu\left(\mathrm{dev}\overline{\mathbf{b}}^{\mathrm{e}}\otimes\mathbf{I} + \mathbf{I}\otimes\mathrm{dev}\overline{\mathbf{b}}^{\mathrm{e}}\right)$$

$$\overline{\mathbb{C}}^{\mathrm{e}}_{\mathrm{f}} = 4\sum_{\alpha\in\mathscr{B}}\left\{\frac{1}{3}\psi^{\alpha}\left[a^{\alpha\alpha}(\mathbb{I} + \frac{1}{3}\mathbf{I}\otimes\mathbf{I}) - (\mathbf{a}^{\alpha}\otimes\mathbf{a}^{\alpha})\otimes\mathbf{I} - \mathbf{I}\otimes(\mathbf{a}^{\alpha}\otimes\mathbf{a}^{\alpha})\right]\right.$$
$$\left. + \psi^{\alpha\alpha}\mathrm{dev}(\mathbf{a}^{\alpha}\otimes\mathbf{a}^{\alpha})\otimes\mathrm{dev}(\mathbf{a}^{\alpha}\otimes\mathbf{a}^{\alpha})\right\}$$

Plastic contributions to the isochoric moduli $\overline{\mathbb{C}}$

$$\overline{\mathbb{C}}^{\mathrm{p}}_{\mathrm{gs}} = 2\sum_{\alpha\in\mathscr{A}}\left(\frac{\partial\tilde{\boldsymbol{\tau}}_{\mathrm{gs}}}{\partial\gamma^{\alpha}}\otimes\sum_{\beta\in\mathscr{A}}G^{\alpha\beta-1}\frac{\partial\hat{\boldsymbol{\Phi}}^{\beta}}{\partial\mathbf{g}}\right), \quad \overline{\mathbb{C}}^{\mathrm{p}}_{\mathrm{f}} = 2\sum_{\mu\in\mathscr{B}}\left[\sum_{\alpha\in\mathscr{A}}\left(\frac{\partial\tilde{\boldsymbol{\tau}}^{\mu}_{\mathrm{f}}}{\partial\gamma^{\alpha}}\otimes\sum_{\beta\in\mathscr{A}}G^{\alpha\beta-1}\frac{\partial\hat{\boldsymbol{\Phi}}^{\beta}}{\partial\mathbf{g}}\right)\right]$$

$$\frac{\partial\tilde{\boldsymbol{\tau}}_{\mathrm{gs}}}{\partial\gamma^{\alpha}} = -\mu\,\mathrm{dev}\left[2\left(\mathbf{a}^{\alpha\,\mathrm{tr}}\otimes\mathbf{a}^{\alpha\,\mathrm{tr}} - \frac{1}{3}\overline{\mathbf{b}}^{\mathrm{e\,tr}}\right)\right.$$
$$\left. - 2\sum_{\beta\in\mathscr{A}}\gamma^{\beta}\left(A^{\alpha\beta}\mathbf{a}^{\alpha\,\mathrm{tr}}\otimes\mathbf{a}^{\beta\,\mathrm{tr}} - \frac{1}{3}\mathbf{a}^{\alpha\,\mathrm{tr}}\otimes\mathbf{a}^{\alpha\,\mathrm{tr}} - \frac{1}{3}\mathbf{a}^{\beta\,\mathrm{tr}}\otimes\mathbf{a}^{\beta\,\mathrm{tr}} + \frac{1}{9}\overline{\mathbf{b}}^{\mathrm{e\,tr}}\right)\right], \quad \alpha\in\mathscr{A}$$

$$\frac{\partial\tilde{\boldsymbol{\tau}}^{\mu}_{\mathrm{f}}}{\partial\gamma^{\alpha}} = 4\psi^{\mu\mu}\left(\mathbf{a}^{\mu}\cdot\frac{\partial\mathbf{a}^{\mu}}{\partial\gamma^{\alpha}}\right)\mathrm{dev}(\mathbf{a}^{\mu}\otimes\mathbf{a}^{\mu}) + 2\psi^{\mu}\mathrm{dev}\left(\mathbf{a}^{\mu}\otimes\frac{\partial\mathbf{a}^{\mu}}{\partial\gamma^{\alpha}} + \frac{\partial\mathbf{a}^{\mu}}{\partial\gamma^{\alpha}}\otimes\mathbf{a}^{\mu}\right), \quad \alpha\in\mathscr{A},\ \ \mu\in\mathscr{B}$$

$$\frac{\partial\hat{\boldsymbol{\Phi}}^{\beta}}{\partial\mathbf{g}} = \mu\ \mathrm{dev}\left(\mathbf{a}^{\beta}\otimes\mathbf{a}^{\beta} - \frac{1}{3}\overline{\mathbf{b}}^{\mathrm{e}}\right) + 2\mathrm{dev}\sum_{\nu\in\mathscr{B}}\left\{\psi^{\nu\nu}\left(A^{\beta\nu}a^{\beta\nu} - \frac{1}{3}a^{\nu\nu}\right)(\mathbf{a}^{\nu}\otimes\mathbf{a}^{\nu})\right.$$
$$\left. + \psi^{\nu}\left[\frac{1}{2}A^{\beta\nu}(\mathbf{a}^{\beta}\otimes\mathbf{a}^{\nu} + \mathbf{a}^{\nu}\otimes\mathbf{a}^{\beta}) - \frac{1}{3}\mathbf{a}^{\nu}\otimes\mathbf{a}^{\nu}\right]\right\}, \quad \beta\in\mathscr{A}$$

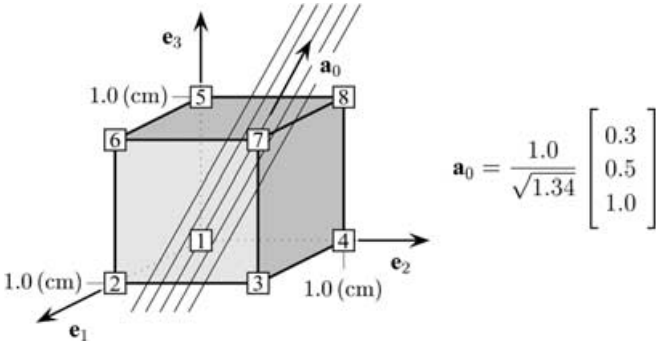

Fig. 4. Reference configuration of a cube and orientation $\mathbf{a}_0$ of the fiber reinforcement and the slip-system

Table 1. Material parameters for the deformation of a single brick

Elastic	Plastic
$\mu = 27.0$ (kPa)	$\tau_0 = 130.0$ (kPa)
$k_1 = 1.28$ (kPa)	$h = 50.0$ (kPa)
$k_2 = 3.54$ $(-)$	$\tau_{0,\infty} = 200.0$ (kPa)
	$a_0 = 0.1$ $(-)$

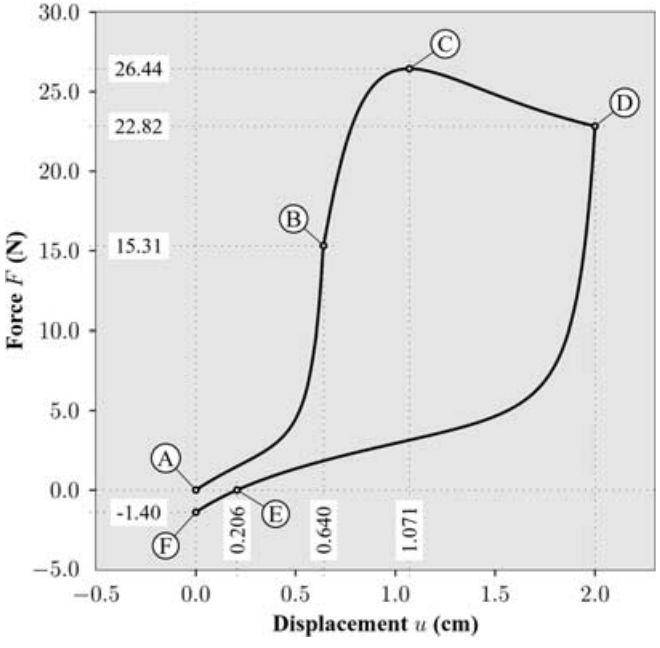

Fig. 5. Evolution of the force F and the displacement u

plastic domain. It demonstrates the applicability of the introduced constitutive framework and numerical algorithm to moderate scale finite element problems. We used an assumed enhanced finite element formulation (EAS) known as $QM1/E12$-element [49], because of its good performance in localization dominated problems. The analysis was carried out on a Pentium IV PC under the

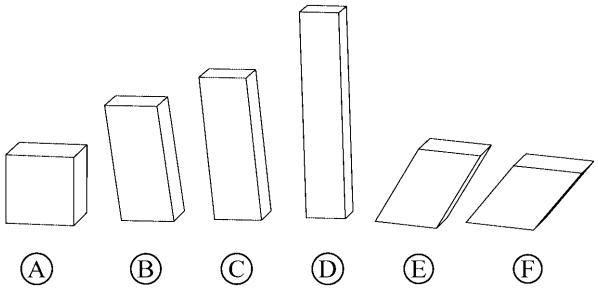

Fig. 6. Configurations at different states of deformation

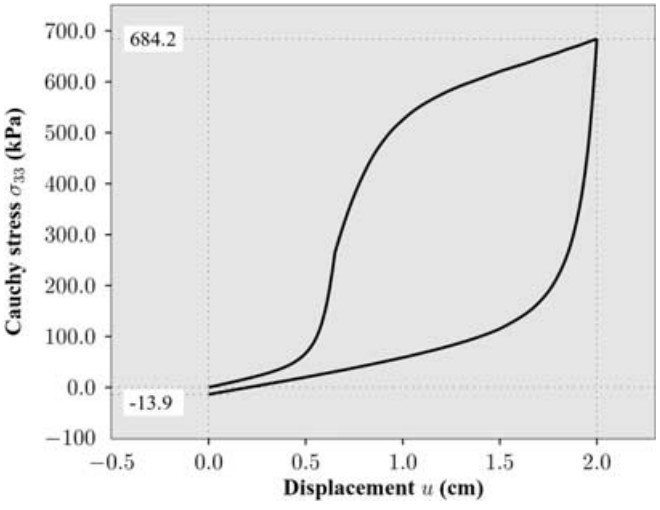

Fig. 7. Evolution of the σ_{33} component of the Cauchy stress with respect to the displacement u. Note that the Cauchy stress monotonically increases during loading

WIN2000 operating system. Symmetries in geometry and loading have been assumed so that only one eighth of the bar and appropriate boundary conditions have been considered. In Fig. 8 the used referential geometry (one eighth of the bar) is shown. In view of material stability investigations a (small) perturbation of the rectangular cylindrical geometry, characterized by the value δ, has been considered. It initializes a necking zone during the extension process. The bar is reinforced by two families of fibers, with fiber angle α as illustrated in Fig. 8. Hence, two independent slip systems are modeled, associated with the two families of fibers.

We apply the set of material parameters as given in Table 4, where, for simplicity, linear hardening is considered.

In order to investigate the evolution of the plastic deformation during extension, the distribution of the hardening variable A of the (whole) bar at different states of extension is shown in Fig. 9. The illustrated three-dimensional computation uses 3240 finite elements for one eighth of the bar, while Fig. 9(a) shows the reference configuration.

Figure 9(b) shows the hardening variable A at a displacement of $u = 2.55$ cm. At this state slightly plastic deformations are present. They are initiated by the introduced geometrical imperfection δ in the middle of the bar. In Fig. 9(c), at the (final) displacement of $u = 6.5$ cm,

Table 2. Convergence of the Newton-Raphson iteration. Residual norm which occurs during the load step from $u = 1.8$ cm to $u = 2.0$ cm

It.-Step	Residual Norm
1	6.48E+02
2	3.35E+01
3	1.14E−01
4	1.91E−02
5	3.73E−06
6	7.99E−11

Table 3. Nodal coordinates at displacement $u = 2.0$ cm

Node	x_1 cm	x_2 cm	x_3 cm
1	0.00E+00	0.00E+00	0.00E+00
2	5.86E−01	0.00E+00	0.00E+00
3	5.55E−01	5.69E−01	0.00E+00
4	−3.11E−02	5.69E−01	0.00E+00
5	−6.21E−02	−1.10E−01	3.00E+00
6	5.24E−01	−1.10E−01	3.00E+00
7	4.93E−01	4.58E−01	3.00E+00
8	−9.32E−02	4.58E−01	3.00E+00

a very well pronounced necking zone can be seen. The figure shows localization of plastic strains in terms of the hardening variable A. A further increase of stretch leads to a softening response, as it was observed in the first example. This phenomenon is accompanied by a strain-localization instability and ('pathological') mesh-dependent solutions, which might be caused by the loss of ellipticity of the governing equations [52]. Furthermore, in Fig. 9(c) we see that plastic deformation in the necking zone accumulates on two sides of the bar. Plastic deformation is not distributed uniformly across the cross-section. This seems to be a typical effect of the anisotropic constitutive formulation and is in contrast to isotropic elastoplastic considerations.

In Fig. 10 the calculated load-displacement curve of one eighth of the bar is plotted. As expected, the extension response starts with a (nonlinear) elastic region until a displacement of about $u = 2.3$ cm is reached. At this state plastic deformation starts to evolve. During a further increase of stretch the tangent of the load-displacement curve decreases. Finally, strain-localization instability leads to a decrease of the load and no quasi-static solutions can be found. In order to deal with this phenomena, we associate the specimen with mass and apply the Newmark transient solution technique. A density of the material of 10^3 kg/m^3 is used. The problem has been assumed to be displacement driven, and each node of the top of the bar moves 0.1 cm per second in the x_3-direction.

In order to investigate the influence of the finite element discretization on the solution, we use four different (structured) finite element meshes. In Fig. 10 the load displacement curves of the different calculations are plotted; the thin line shows the response of the geometrical perfect bar ($\delta = 0.0$), while the thick lines are associated with the imperfect geometries ($\delta = 0.05$ cm). We used the material parameters given in Table 4, where for simplicity

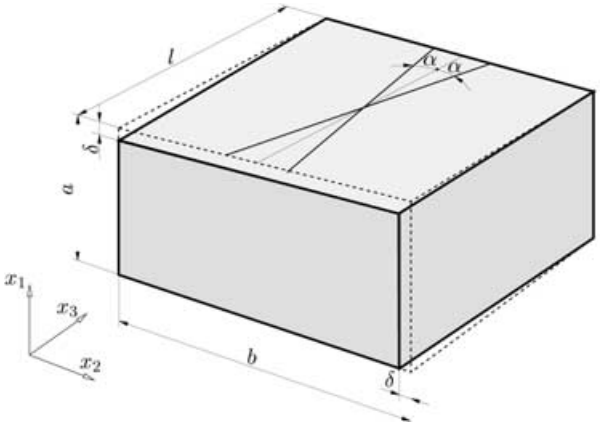

Geometry

a =	2.0 (cm)
b =	5.0 (cm)
l =	7.0 (cm)
δ =	0.05 (cm)

Arrangement of the families of fibers

α =	7.0 (°)

Fig. 8. Referential geometry and structural arrangement of two families of fibers of one eighth of a bar. A (small) perturbation of the rectangular cylindrical geometry is characterized by the value δ

Table 4. Material parameters for the necking problem

Elastic	Plastic
$\mu = 30.0$ (kPa)	$\tau_0 = 70.0$ (kPa)
$k_1 = 4.0$ (kPa)	$h = 100.0$ (kPa)
$k_2 = 2.3$ $(-)$	

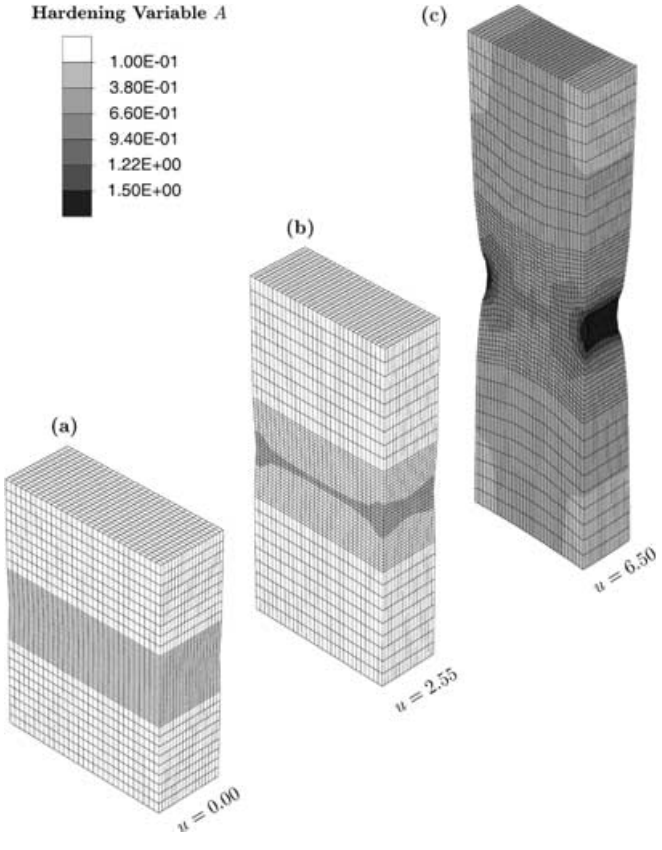

Fig. 9. Evolution of the plastic deformation in terms of the hardening variable A during extension. (a) Reference configuration; (b) exceeding elastic limit and evolution of plastic deformation; (c) pronounced localization of plastic deformation accumulated at two sides of the bar

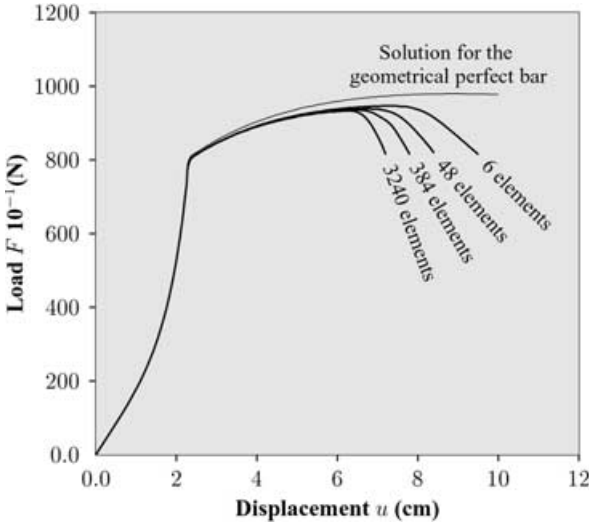

Fig. 10. Comparison of the load displacement curves achieved with different finite element discretizations. The thin line shows the mechanical response of the geometrical perfect bar. The thick lines are associated with imperfect geometries, discretized with 6, 48, 384 and 3240 finite elements. At the elastic limit the yield stress is reached and plastic deformation starts to evolve. At a certain (discretization based) displacement a strain-localization instability appears which leads to typical mesh-dependent solution

only linear hardening is assumed, and utilized FE discretizations with 6, 48, 384 and 3240 finite elements. The constitutive formulation in conjunction with the used material parameters lead to a softening response (similar to Fig. 5) at a certain (discretization based) displacement u. This leads to an immediate decrease of the load and, without regularization, to the typical mesh-dependent solutions, as known from the literature, see for example Zienkiewicz and Taylor [61] and references therein. It is well known that strain localization caused by strain-softening leads to physically meaningless results using a local continuum theory. This theory predicts zero dissipation at failure and a finite element calculation attempts to converge to this meaningless solution [5]. In order to avoid this spurious mesh sensitivity, the model could, for example, be viscoregularized [10] or extended to a nonlocal fashion by introducing a characteristic length [41]. The use

of a Cosserat continuum [8] or gradient plasticity [10] are also useful; they are more advanced methods in order to avoid mesh sensitivity.

Note that in view of the above discussed problems the results obtained for the softening region are questionable. As far as soft biological tissues are concerned the solid material is often penetrated by a fluid. More advanced constitutive models, which incorporate viscosities, may avoid the 'pathological' solutions.

Although we used the advanced $QM1/E12$ formulation the deformed meshes are accompanied with hourglass modes, see Fig. 9(c).

6 Conclusion

In this paper a framework of finite strain rate-independent multisurface plasticity for fiber-reinforced composites has been developed. In particular, we focused attention on modeling soft biological tissues in a supra-physiological loading domain and employed the continuum theory of the mechanics of fiber-reinforced composites, [54], by neglecting coupling phenomena. The chosen (macroscopic) continuum theory is based on a multiplicative decomposition of the deformation gradient into elastic and plastic parts.

The elastic part of the deformation is described by an anisotropic Helmholtz free-energy function, which captures elastic arterial deformations particularly well. The free energy has several advantages over alternative descriptions known in the literature (for a comparison see [21]), although only a relatively small number of material parameters are needed for describing the three-dimensional case. A further advantage of the suggested free energy is the fact that the structural architecture of the composite may be correlated with the material parameters.

The kinematics of the plastic deformation is described by means of the plastic part $\mathbf{L}^{\mathrm{p}}$ of $\mathbf{L}$, which is a rate tensor obtained from the transformation of the spatial velocity gradient $\mathbf{l}$ to the intermediate configuration. An elastic domain – bounded by a convex, but non-smooth yield surface – is defined by n-independent (nonredundant) yield criterion functions, which follow the concept of multisurface plasticity. It is shown that the plastic dissipation for the model is always non-negative, which is in accordance with the second law of thermodynamics.

The numerical implementation of the constitutive framework is based on the (backward-Euler) integration of the flow rule and the commonly used elastic predictor/plastic corrector concept to update the plastic variables. In particular, two alternative plastic corrector schemes are formulated (direct and indirect methods) satisfying the yield criterion functions by the Karush-Kuhn-Tucker conditions. The indirect method, which only involves equations, turns out to be advantageous in the sense that the plastic corrector procedure works without estimating the set of active slip systems. The stress response and the novel consistent linearized elastoplastic moduli are derived explicitly in a geometric setting relative to the current configuration. The closed-form expressions have been implemented in the multi-purpose finite element analysis program FEAP.

In order to investigate the proposed material model in more detail, two representative numerical examples have been analyzed. The first example considers a fiber-reinforced cube modeled by one 8-node $Q1/P0$-element. The displacement-driven computation shows the basic inelastic features such as (plastic) hysteresis and residual strains. In addition, the robustness of the numerical concept and the accuracy of the numerical integration of the evolution equations were studied. The second example shows the applicability of the constitutive formulation to moderate scale finite element problems. It studies the elastoplastic extension of geometrical perfect and imperfect rectangular bars. Exceeding the elastic limit a pronounced localization of the plastic deformation evolved. After a certain (discretization based) displacement the calculation led to strain-localization instability and the typically spurious mesh sensitive solution.

The proposed concept is the first application of multisurface plasticity to fiber-reinforced composites. It incorporates structural information of the material and approaches the complex deformation problem from an engineering point of view with the goal of achieving a meaningful and efficient numerical realization. The constitutive theory can easily be extended for incorporating viscous phenomena [20].

Appendix A. Kirchhoff stresses and Eulerian elasticity tensor due to $\bar{\Psi}_{\mathrm{f}}^{\alpha}$

A.1: Derivation of formula $(47)_3$

From the anisotropic free-energy function $\bar{\Psi}_{\mathrm{f}}^{\alpha}$, $\alpha = 1, \ldots, n$, we may derive the second Piola-Kirchhoff stress tensors $\bar{\mathbf{S}}_{\mathrm{f}}^{\alpha}$, which we define as

$$\bar{\mathbf{S}}_{\mathrm{f}}^{\alpha} = 2\frac{\partial \bar{\Psi}_{\mathrm{f}}^{\alpha}(\bar{I}_4^{\alpha})}{\partial \mathbf{C}^{\mathrm{e}}} = 2\psi^{\alpha}\frac{\partial \bar{I}_4^{\alpha}}{\partial \mathbf{C}^{\mathrm{e}}}, \quad \alpha \in \mathscr{B} \ , \tag{87}$$

where $\bar{I}_4^{\alpha} = \bar{\mathbf{C}}^{\mathrm{e}} : \mathbf{a}_0^{\alpha} \otimes \mathbf{a}_0^{\alpha}$ are invariants, $\psi^{\alpha} = \partial \bar{\Psi}_{\mathrm{f}}^{\alpha}/\partial \bar{I}_4^{\alpha}$ are stress functions and $\mathscr{B}$ denotes the set of stretched fibers. Note that the symmetric stress tensors $\bar{\mathbf{S}}_{\mathrm{f}}^{\alpha}$ are parameterized by coordinates which are referred to the macro-stress-free intermediate configuration (see Sect. 2.1).

Now we need to compute the partial derivative of $\bar{I}_4^{\alpha}$ with respect to the elastic right Cauchy-Green tensor $\mathbf{C}^{\mathrm{e}}$. By means of the properties (33), $(44)_2$, the chain rule and the fact that $\partial \bar{I}_4^{\alpha}/\partial \bar{\mathbf{C}}^{\mathrm{e}} = \mathbf{a}_0^{\alpha} \otimes \mathbf{a}_0^{\alpha}$, we obtain

$$\begin{aligned}\frac{\partial \bar{I}_4^{\alpha}}{\partial \mathbf{C}^{\mathrm{e}}} &= \frac{\partial \bar{I}_4^{\alpha}}{\partial \bar{\mathbf{C}}^{\mathrm{e}}} : \frac{\partial \bar{\mathbf{C}}^{\mathrm{e}}}{\partial \mathbf{C}^{\mathrm{e}}} = J^{-2/3}\left(\mathbf{a}_0^{\alpha} \otimes \mathbf{a}_0^{\alpha} - \frac{1}{3}\bar{I}_4^{\alpha}\bar{\mathbf{C}}^{\mathrm{e}-1}\right) \\ &= J^{-2/3}\mathrm{Dev}\left(\mathbf{a}_0^{\alpha} \otimes \mathbf{a}_0^{\alpha}\right) \ ,\end{aligned} \tag{88}$$

where we have introduced the deviatoric operator $\mathrm{Dev}(\bullet) = (\bullet) - (1/3)\left[(\bullet) : \bar{\mathbf{C}}^{\mathrm{e}}\right]\bar{\mathbf{C}}^{\mathrm{e}-1}$. By means of $(88)_3$, we obtain from $(87)_2$ the second Piola-Kirchhoff stress tensors

$$\bar{\mathbf{S}}_{\mathrm{f}}^{\alpha} = 2J^{-2/3}\psi^{\alpha}\mathrm{Dev}\left(\mathbf{a}_0^{\alpha} \otimes \mathbf{a}_0^{\alpha}\right), \alpha \in \mathscr{B} \ . \tag{89}$$

A push-forward operation transforms $\bar{\mathbf{S}}_{\mathrm{f}}^{\alpha}$ to the current configuration to give the associated isochoric Kirchhoff stress tensors

$$\tilde{\boldsymbol{\tau}}_{\mathrm{f}}^{\alpha} = \mathbf{F}^{\mathrm{e}}\bar{\mathbf{S}}_{\mathrm{f}}^{\alpha}\mathbf{F}^{\mathrm{eT}} = 2J^{-2/3}\psi^{\alpha}\mathbf{F}^{\mathrm{e}}\left(\mathbf{a}_0^{\alpha}\otimes\mathbf{a}_0^{\alpha} - \frac{1}{3}\bar{I}_4^{\alpha}\bar{\mathbf{C}}^{\mathrm{e}-1}\right)\bar{\mathbf{F}}^{\mathrm{e}}, \quad \alpha\in\mathscr{B} \ . \tag{90}$$

Finally, with $\mathbf{F}^{\mathrm{e}} = J^{1/3}\bar{\mathbf{F}}^{\mathrm{e}}$, $\mathbf{a}^{\alpha} = \bar{\mathbf{F}}^{\mathrm{e}}\mathbf{a}_0^{\alpha}$ and the relations $\bar{I}_4^{\alpha} = \mathbf{a}^{\alpha}\cdot\mathbf{a}^{\alpha} = (\mathbf{a}^{\alpha}\otimes\mathbf{a}^{\alpha}) : \mathbf{I}$ we find that $\tilde{\boldsymbol{\tau}}_{\mathrm{f}}^{\alpha} = 2\psi^{\alpha}\mathrm{dev}(\mathbf{a}^{\alpha}\otimes\mathbf{a}^{\alpha})$, $\alpha\in\mathscr{B}$, which establishes Eq. $(47)_3$. Here we have used property (16) for the deviatoric operator in the Eulerian description.

A.2: Derivation of formula (76)

We introduce the elasticity tensor $\bar{\mathbb{C}}_{\mathrm{f}}^{\mathrm{e}}$ as the gradient of the nonlinear function $\bar{\mathbf{S}}_{\mathrm{f}}$ according to

$$\bar{\mathbb{C}}_{\mathrm{f}}^{\mathrm{e}} = 2\sum_{\alpha\in\mathscr{B}}\frac{\partial\bar{\mathbf{S}}_{\mathrm{f}}^{\alpha}}{\partial\mathbf{C}^{\mathrm{e}}} \ . \tag{91}$$

The fourth-order tensor $\bar{\mathbb{C}}_{\mathrm{f}}^{\mathrm{e}}$ is parameterized by coordinates which are referred to the intermediate configuration.

Before we start to derive the closed-form expression for the elasticity tensor we determine the partial derivative of $\mathrm{Dev}\left(\mathbf{a}_0^{\alpha}\otimes\mathbf{a}_0^{\alpha}\right)$ with respect to $\mathbf{C}^{\mathrm{e}}$. By means of $(88)_2$, the chain rule and $(88)_3$, we find that

$$\frac{\partial\mathrm{Dev}\left(\mathbf{a}_0^{\alpha}\otimes\mathbf{a}_0^{\alpha}\right)}{\partial\mathbf{C}^{\mathrm{e}}} = -\frac{1}{3}\left(J^{-2/3}\bar{\mathbf{C}}^{\mathrm{e}-1}\otimes\mathrm{Dev}\left(\mathbf{a}_0^{\alpha}\otimes\mathbf{a}_0^{\alpha}\right) + \bar{I}_4^{\alpha}\frac{\partial\bar{\mathbf{C}}^{\mathrm{e}-1}}{\partial\bar{\mathbf{C}}^{\mathrm{e}}} : \frac{\partial\bar{\mathbf{C}}^{\mathrm{e}}}{\partial\mathbf{C}^{\mathrm{e}}}\right) . \tag{92}$$

Hence, with $(44)_2$, the fact that $\partial\bar{\mathbf{C}}^{\mathrm{e}-1}/\partial\bar{\mathbf{C}}^{\mathrm{e}} : \bar{\mathbf{C}}^{\mathrm{e}}\otimes\bar{\mathbf{C}}^{\mathrm{e}-1} = -\bar{\mathbf{C}}^{\mathrm{e}-1}\otimes\bar{\mathbf{C}}^{\mathrm{e}-1}$, and the property $(4)_1$, we obtain

$$\frac{\partial\mathrm{Dev}\left(\mathbf{a}_0^{\alpha}\otimes\mathbf{a}_0^{\alpha}\right)}{\partial\mathbf{C}^{\mathrm{e}}} = -\frac{1}{3}[\mathbf{C}^{\mathrm{e}-1}\otimes\mathrm{Dev}\left(\mathbf{a}_0^{\alpha}\otimes\mathbf{a}_0^{\alpha}\right) - J^{2/3}\bar{I}_4^{\alpha}(\mathbf{C}^{\mathrm{e}-1}\odot\mathbf{C}^{\mathrm{e}-1} - \frac{1}{3}\mathbf{C}^{\mathrm{e}-1}\otimes\mathbf{C}^{\mathrm{e}-1})] \ . \tag{93}$$

Here, for convenience, we have introduced the definition

$$\frac{\partial\mathbf{C}^{\mathrm{e}-1}}{\partial\mathbf{C}^{\mathrm{e}}} = -\mathbf{C}^{\mathrm{e}-1}\odot\mathbf{C}^{\mathrm{e}-1} \tag{94}$$

of the fourth-order tensor $\partial\mathbf{C}^{\mathrm{e}-1}/\partial\mathbf{C}^{\mathrm{e}}$, where the symbol $\odot$ denotes the tensor product according to the rule [19]

$$-(\mathbf{C}^{\mathrm{e}-1}\odot\mathbf{C}^{\mathrm{e}-1})_{IJKL} = -\frac{1}{2}(C_{IK}^{\mathrm{e}-1}C_{JL}^{\mathrm{e}-1} + C_{JK}^{\mathrm{e}-1}C_{IL}^{\mathrm{e}-1}) = \frac{\partial C_{IJ}^{\mathrm{e}-1}}{\partial C_{KL}^{\mathrm{e}}} \ . \tag{95}$$

Using Eq. (89) and the chain rule, the elasticity tensor $\bar{\mathbb{C}}_{\mathrm{f}}^{\mathrm{e}}$ follows from the definition (91) as

$$\bar{\mathbb{C}}_{\mathrm{f}}^{\mathrm{e}} = 4\sum_{\alpha\in\mathscr{B}}\left[\psi^{\alpha}\mathrm{Dev}\left(\mathbf{a}_0^{\alpha}\otimes\mathbf{a}_0^{\alpha}\right)\otimes\frac{\partial J^{-2/3}}{\partial\mathbf{C}^{\mathrm{e}}} + J^{-2/3}\mathrm{Dev}\left(\mathbf{a}_0^{\alpha}\otimes\mathbf{a}_0^{\alpha}\right)\otimes\frac{\partial\psi^{\alpha}}{\partial\mathbf{C}^{\mathrm{e}}} + J^{-2/3}\psi^{\alpha}\frac{\mathrm{Dev}\left(\mathbf{a}_0^{\alpha}\otimes\mathbf{a}_0^{\alpha}\right)}{\partial\mathbf{C}^{\mathrm{e}}}\right] , \tag{96}$$

and with properties $(44)_1$, $(88)_3$, (93), we obtain, after recasting,

$$\bar{\mathbb{C}}_{\mathrm{f}}^{\mathrm{e}} = 4\sum_{\alpha\in\mathscr{B}}\left\{\frac{1}{3}\psi^{\alpha}[\bar{I}_4^{\alpha}(\mathbf{C}^{\mathrm{e}-1}\odot\mathbf{C}^{\mathrm{e}-1} - \frac{1}{3}\mathbf{C}^{\mathrm{e}-1}\otimes\mathbf{C}^{\mathrm{e}-1}) - J^{-2/3}\mathrm{Dev}\left(\mathbf{a}_0^{\alpha}\otimes\mathbf{a}_0^{\alpha}\right)\otimes\mathbf{C}^{\mathrm{e}-1} - J^{-2/3}\mathbf{C}^{\mathrm{e}-1}\otimes\mathrm{Dev}\left(\mathbf{a}_0^{\alpha}\otimes\mathbf{a}_0^{\alpha}\right)] + J^{-4/3}\psi^{\alpha\alpha}\mathrm{Dev}\left(\mathbf{a}_0^{\alpha}\otimes\mathbf{a}_0^{\alpha}\right)\otimes\mathrm{Dev}\left(\mathbf{a}_0^{\alpha}\otimes\mathbf{a}_0^{\alpha}\right)\right\} , \tag{97}$$

with the elasticity functions $\psi^{\alpha\alpha} = \mathrm{d}^2\bar{\Psi}_{\mathrm{f}}^{\alpha}/\mathrm{d}\bar{I}_4^{\alpha}\mathrm{d}\bar{I}_4^{\alpha}$, $\alpha\in\mathscr{B}$. Finally, by means of $(88)_2$ and $(4)_1$ we find the closed-form expression

$$\bar{\mathbb{C}}_{\mathrm{f}}^{\mathrm{e}} = 4\sum_{\alpha\in\mathscr{B}}\left\{\frac{1}{3}\psi^{\alpha}[\bar{I}_4^{\alpha}(\mathbf{C}^{\mathrm{e}-1}\odot\mathbf{C}^{\mathrm{e}-1} + \frac{1}{3}\mathbf{C}^{\mathrm{e}-1}\otimes\mathbf{C}^{\mathrm{e}-1}) - J^{-2/3}\left(\mathbf{a}_0^{\alpha}\otimes\mathbf{a}_0^{\alpha}\right)\otimes\mathbf{C}^{\mathrm{e}-1} - J^{-2/3}\mathbf{C}^{\mathrm{e}-1}\otimes\left(\mathbf{a}_0^{\alpha}\otimes\mathbf{a}_0^{\alpha}\right)] + J^{-4/3}\psi^{\alpha\alpha}\mathrm{Dev}(\mathbf{a}_0^{\alpha}\otimes\mathbf{a}_0^{\alpha})\otimes\mathrm{Dev}(\mathbf{a}_0^{\alpha}\otimes\mathbf{a}_0^{\alpha})\right\} . \tag{98}$$

The associated Eulerian description of the elasticity tensor is found by a push-forward operation of $\bar{\mathbb{C}}_{\mathrm{f}}^{\mathrm{e}}$ to the current configuration. This operation may be written in index notation as

$$(\bar{\mathbb{c}}_{\mathrm{f}}^{\mathrm{e}})_{ijkl} = F_{iI}^{\mathrm{e}}F_{jJ}^{\mathrm{e}}F_{kK}^{\mathrm{e}}F_{lL}^{\mathrm{e}}(\bar{\mathbb{C}}_{\mathrm{f}}^{\mathrm{e}})_{IJKL} \ . \tag{99}$$

To specify this transformation we use relation $(4)_1$, the definition of the deviatoric operator (16) in the Eulerian description and the map $\mathbf{a}^{\alpha} = \bar{\mathbf{F}}^{\mathrm{e}}\mathbf{a}_0^{\alpha}$. Hence, based on (99), the Eulerian elasticity tensor $\bar{\mathbb{c}}_{\mathrm{f}}^{\mathrm{e}}$ reads

$$\bar{\mathbb{c}}_{\mathrm{f}}^{\mathrm{e}} = 4\sum_{\alpha\in\mathscr{B}}\left\{\frac{1}{3}\psi^{\alpha}[\bar{I}_4^{\alpha}(\mathbb{I} + \frac{1}{3}\mathbf{I}\otimes\mathbf{I}) - (\mathbf{a}^{\alpha}\otimes\mathbf{a}^{\alpha})\otimes\mathbf{I} - \mathbf{I}\otimes(\mathbf{a}^{\alpha}\otimes\mathbf{a}^{\alpha})] + \psi^{\alpha\alpha}\mathrm{dev}(\mathbf{a}^{\alpha}\otimes\mathbf{a}^{\alpha})\otimes\mathrm{dev}(\mathbf{a}^{\alpha}\otimes\mathbf{a}^{\alpha})\right\} ,$$

which is the desired result (76).

Appendix B. Eulerian elasticity tensor $\bar{\mathbb{c}}_{\mathrm{gs}}^{\mathrm{p}}$

Here we derive expressions necessary for the computation of the plastic part $\bar{\mathbb{c}}_{\mathrm{gs}}^{\mathrm{p}}$ of the elasticity tensor defined in Eq. $(77)_1$. In particular, we specify the terms $\partial\tilde{\boldsymbol{\tau}}_{\mathrm{gs}}/\partial\gamma^{\alpha}$ and $\partial\hat{\boldsymbol{\Phi}}^{\alpha}/\partial\mathbf{g}$, the latter being used for computing $\partial\gamma^{\alpha}/\partial\mathbf{g}$.

B.1: Derivation of formula (79)

First let us introduce the property $\partial(\mathrm{dev}\bar{\mathbf{b}}^{\mathrm{e}})/\partial\gamma^{\alpha} = \mathrm{dev}(\partial\bar{\mathbf{b}}^{\mathrm{e}}/\partial\gamma^{\alpha})$. Hence, from stress relation $(47)_2$ we may obtain the derivative of $\tilde{\boldsymbol{\tau}}_{\mathrm{gs}}$ with respect to the incremental slip parameters γ^{α}, i.e.

$$\frac{\partial \tilde{\boldsymbol{\tau}}_{\mathrm{gs}}}{\partial \gamma^{\alpha}} = \mu \mathrm{dev}\left(\frac{\partial \bar{\mathbf{b}}^{\mathrm{e}}}{\partial \gamma^{\alpha}}\right) \ , \tag{100}$$

as is required for $(77)_1$. All that remains is the explicit expression for $\partial \bar{\mathbf{b}}^{\mathrm{e}}/\partial \gamma^{\alpha}$. From the derivation of the algorithmic expression (78) it is straightforward to obtain

$$\begin{aligned}\frac{\partial \bar{\mathbf{b}}^{\mathrm{e}}}{\partial \gamma^{\alpha}} = &-2\left(\mathbf{a}^{\alpha\,\mathrm{tr}} \otimes \mathbf{a}^{\alpha\,\mathrm{tr}} - \frac{1}{3}\bar{\mathbf{b}}^{\mathrm{e}\,\mathrm{tr}}\right) \\ &+ 2\sum_{\beta \in \mathscr{A}} \gamma^{\beta}\left(A^{\alpha\beta}\mathbf{a}^{\alpha\,\mathrm{tr}} \otimes \mathbf{a}^{\beta\,\mathrm{tr}} - \frac{1}{3}\mathbf{a}^{\alpha\,\mathrm{tr}} \otimes \mathbf{a}^{\alpha\,\mathrm{tr}}\right. \\ &\left. - \frac{1}{3}\mathbf{a}^{\beta\,\mathrm{tr}} \otimes \mathbf{a}^{\beta\,\mathrm{tr}} + \frac{1}{9}\bar{\mathbf{b}}^{\mathrm{e}\,\mathrm{tr}}\right),\end{aligned} \tag{101}$$

which, together with (100), gives the desired formula (79).

B.2: Derivation of formula (81)

Before we start to derive formula (81) it is necessary to differentiate the coefficients $a^{\alpha\beta}$ with respect to the Eulerian metric $\mathbf{g}$. Use of Eqs. $(37)_1$, (36) and $(4)_3$, and successive application of the chain rule gives

$$\frac{\partial a^{\alpha\beta}}{\partial \mathbf{g}} = \frac{\partial(\bar{\mathbf{C}}^{\mathrm{e}} : \mathbf{a}_0^{\alpha} \otimes \mathbf{a}_0^{\beta})}{\partial \mathbf{g}} = \frac{\partial(\bar{\mathbf{C}}^{\mathrm{e}} : \mathbf{a}_0^{\alpha} \otimes \mathbf{a}_0^{\beta})}{\partial \bar{\mathbf{C}}^{\mathrm{e}}} : \frac{\partial \bar{\mathbf{C}}^{\mathrm{e}}}{\partial \mathbf{C}^{\mathrm{e}}} : \frac{\partial \mathbf{C}^{\mathrm{e}}}{\partial \mathbf{g}} \ . \tag{102}$$

Hence, by means of the fourth-order unit tensor $(\mathbb{I})_{IJKL} = (\delta_{IK}\delta_{JL} + \delta_{IL}\delta_{JK})/2$, the term $\partial(\bar{\mathbf{C}}^{\mathrm{e}} : \mathbf{a}_0^{\alpha} \otimes \mathbf{a}_0^{\beta})/\partial \bar{\mathbf{C}}^{\mathrm{e}}$ reads

$$\frac{\partial(\bar{\mathbf{C}}^{\mathrm{e}} : \mathbf{a}_0^{\alpha} \otimes \mathbf{a}_0^{\beta})}{\partial \bar{\mathbf{C}}^{\mathrm{e}}} = \mathbb{I} : \mathbf{a}_0^{\alpha} \otimes \mathbf{a}_0^{\beta} = \frac{1}{2}\left(\mathbf{a}_0^{\alpha} \otimes \mathbf{a}_0^{\beta} + \mathbf{a}_0^{\beta} \otimes \mathbf{a}_0^{\alpha}\right) \ , \tag{103}$$

which can be shown by means of index notation.

In order to proceed with the derivation of $\partial a^{\alpha\beta}/\partial \mathbf{g}$, we recall the results $\partial \bar{\mathbf{C}}^{\mathrm{e}}/\partial \mathbf{C}^{\mathrm{e}} = J^{-2/3}(\mathbb{I} - \bar{\mathbf{C}}^{\mathrm{e}} \otimes \bar{\mathbf{C}}^{\mathrm{e}-1}/3)$ and $\partial \mathbf{C}^{\mathrm{e}}/\partial \mathbf{g} = \mathbf{F}^{\mathrm{e}} \odot \mathbf{F}^{\mathrm{e}}$. By using these relations and Eq. $(103)_2$, we find from $(102)_2$ that

$$\begin{aligned}\frac{\partial a^{\alpha\beta}}{\partial \mathbf{g}} = &\frac{1}{2}\left[\mathbf{a}_0^{\alpha} \otimes \mathbf{a}_0^{\beta} + \mathbf{a}_0^{\beta} \otimes \mathbf{a}_0^{\alpha} - \frac{2}{3}\mathrm{tr}(\mathbf{a}^{\alpha} \otimes \mathbf{a}^{\beta})\bar{\mathbf{C}}^{\mathrm{e}-1}\right] \\ &: (\bar{\mathbf{F}}^{\mathrm{e}} \odot \bar{\mathbf{F}}^{\mathrm{e}}) \ ,\end{aligned} \tag{104}$$

where we employed Eqs. (36), $(4)_3$ and the definition of the modified elastic deformation gradient $\bar{\mathbf{F}}^{\mathrm{e}} = J^{-1/3}\mathbf{F}^{\mathrm{e}}$. By recalling Eqs. (36) and $(4)_3$ once more, and by means of the tensor product as defined in $(46)_2$ and the deviatoric operator from (16), we obtain, after some straightforward tensor algebra, the important relation

$$\frac{\partial a^{\alpha\beta}}{\partial \mathbf{g}} = \frac{1}{2}\mathrm{dev}\left(\mathbf{a}^{\alpha} \otimes \mathbf{a}^{\beta} + \mathbf{a}^{\beta} \otimes \mathbf{a}^{\alpha}\right) \ . \tag{105}$$

Here, the tensor manipulations are best performed in index notation. Noting $(38)_2$, we see that Eq. (105) is

$$\frac{\partial \bar{I}_4^{\alpha}}{\partial \mathbf{g}} = \mathrm{dev}(\mathbf{a}^{\alpha} \otimes \mathbf{a}^{\alpha}) \ . \tag{106}$$

Now, for the derivation of formula (81) we need Eqs. (105) and (106) and, in addition, the property $\partial \bar{I}_1/\partial \mathbf{g} = \mathrm{dev}\,\bar{\mathbf{b}}^{\mathrm{e}}$. Hence, from the specified form (31), the scalar measures τ^{α}, as given in (51), and use of the chain rule, we obtain

$$\begin{aligned}\frac{\partial \hat{\boldsymbol{\Phi}}^{\alpha}}{\partial \mathbf{g}} = \frac{\partial \tau^{\alpha}}{\partial \mathbf{g}} = &\mu\,\mathrm{dev}\left(\mathbf{a}^{\alpha} \otimes \mathbf{a}^{\alpha} - \frac{1}{3}\bar{\mathbf{b}}^{\mathrm{e}}\right) \\ &+ 2\mathrm{dev}\sum_{\beta \in \mathscr{B}}\left\{\psi^{\beta\beta}\left(A^{\alpha\beta}a^{\alpha\beta} - \frac{1}{3}a^{\beta\beta}\right)\left(\mathbf{a}^{\beta} \otimes \mathbf{a}^{\beta}\right)\right. \\ &+ \psi^{\beta}\left[\frac{1}{2}A^{\alpha\beta}\left(\mathbf{a}^{\alpha} \otimes \mathbf{a}^{\beta} + \mathbf{a}^{\beta} \otimes \mathbf{a}^{\alpha}\right)\right. \\ &\left.\left. - \frac{1}{3}\mathbf{a}^{\beta} \otimes \mathbf{a}^{\beta}\right]\right\} \ .\end{aligned} \tag{107}$$

A replacement of the dummy indices α in $(107)_2$ by β and β by ν gives the desired result (81).

References

1. **Abrahams M** (1967) Mechanical behaviour of tendon in vitro. A preliminary report. Med. Biol. Eng. 5: 433–443
2. **Asaro RJ** (1983) Crystal plasticity. J. Appl. Mech. 50: 921–934
3. **Asaro RJ** (1983) Micromechancis of crystals and polycrystals. In: Advances in Applied Mechanics, Volume 23. San Diego: Academic Press
4. **Babuška I** (1973) The finite element method with Lagrangian multipliers. Appl. Numer. Math. 20: 179–192
5. **Bažant ZP, Pijaudier-Cabot G** (1988) Nonlocal continuum damage, localization instability and convergence. J. Appl. Mech. 55: 287–293
6. **Bertsekas DP** (1996) Constrained Optimization and Lagrange Multiplier Methods. Belmont: Athena Scientific
7. **Block PC** (1984) Mechanism of transluminal angioplasty. Am. J. Cardiol. 53: 69C–71C
8. **Cosserat E, Cosserat F** (1898) Sur les equations de la theorie de l'elaticite. Comptes Rendus de l'Acad. Sci. Paris, 126: 1129–1132
9. **Crisfield MA** (1997) Non-linear Finite Element Analysis of Solids and Structures, Advanced Topics, Volume 2. Chichester: John Wiley & Sons
10. **de Borst R, Sluys LJ, Hüllhaus HB, Pamin J** (1993) Fundamental issues in finite element analysis of localization of deformation. Engr. Comp. 10: 99–121
11. **Desai CS, Siriwardane HJ** (1984) Constitutive Laws for Engineering Materials. New Jersey: Prentice-Hall, Englewood Cliffs
12. **DiMaggio FL, Sandler IS** (1971) Material model for granular soils. J. Engr. Mech. Div. EM 3: 935–950
13. **Ebers-Ernst J, Dinkler D** (2000) Simulation of deformation behavior of municipal solid waste landfills. Proc. of European Congress on Computational Methods in Applied Sciences and Engineering, ECCOMAS, Barcelona
14. **Emery JL, Omens JH, McCulloch, AD** (1997) Strain softening in rat left ventricular myocardium. J. Biomech. Engr. 119: 6–12
15. **Flory PJ** (1961) Thermodynamic relations for highly elastic materials. Trans. Faraday Soc. 57: 829–838
16. **Fung YC, Fronek K, Patitucci P** (1979) Pseudoelasticity of arteries and the choice of its mathematical expression. Am. J. Physiol. 237: H620–H631
17. **Hill R** (1950) The mathematical theory of plasticity. Oxford: Oxford University Press
18. **Hokanson J, Yazdani S** (1997) A constitutive model of the artery with damage. Mech. Res. Commun. 24: 151–159

19. **Holzapfel GA** (2000) Nonlinear Solid Mechanics. A Continuum Approach for Engineering. Chichester: John Wiley & Sons
20. **Holzapfel GA, Gasser TC** (2001) A viscoelastic model for fiber-reinforced composites at finite strains: Continuum basis, computational aspects and applications. Comput. Meth. Appl. Mech. Engr. 190: 4379–4403
21. **Holzapfel GA, Gasser TC, Ogden RW** (2000) A new constitutive framework for arterial wall mechanics and a comparative study of material models. J. Elasticity, 61: 1–48
22. **Kachanov LM** (1958) Time of the rupture process under creep conditions. Izvestija Akademii Nauk Sojuza Sovetskich Socialisticeskich Respubliki (SSSR) Otdelenie Techniceskich Nauk (Moskra), 8: 26–31
23. **Kahn AS, Huang S** (1995) Continuum Theory of Plasticity. New York: John Wiley & Sons
24. **Kaliske M, Rothert H** (1999) Viscoelastic and elastoplastic damage formulation. In: Dorfmann A, Muhr A (Eds) Constitutive models for rubber, Rotterdam, A. A. Balkema
25. **Ker RF, Wang XT, Pike AVL** (2000) Fatique quality of mammalian tendons. J. Exp. Biol. 203: 1317–1327
26. **Krajcinovic D** (1996) Damage Mechanics. Amsterdam: North-Holland
27. **Liao H, Belkoff SM** (1999) A failure model for ligaments. J. Biomech. 32: 183–188
28. **Lubliner J** (1990) Plasticity Theory. New York: Macmillan Publishing Company
29. **Malvern LE** (1969) Introduction to the Mechanics of a Continuous Medium . Englewood Cliffs New Jersey: Prentice-Hall
30. **Miehe C** (1994) On the representation of prandtl-reuss tensors within the framework of multiplicative plasticity. Int. J. Plasticity 10: 609–621
31. **Miehe C** (1995) Entropic thermoelasticity at finite strains. Aspects of the formulation and numerical implementation. Comput. Meth. Appl. Mech. Engr. 20: 243–269
32. **Miehe C** (1996) Multisurface thermoplasticity for single crystals at large strains in terms of Eulerian vector updates. Int. J. Solids and Structures 33: 3103–3130
33. **Miehe C** (1996) Numerical computation of algorithmic (consistent) tangent moduli in large-strain computational inelasticity. Comput. Meth. Appl. Mech. Engr. 134: 223–240
34. **Miehe C, Schröder J** (2001) A comparative study of stress update algorithms for rate-independent and rate-dependent crystal plasticity. Int. J. Numer. Meth. Engr. 50: 273–298
35. **Moreau JJ** (1976) Application of convex analysis to the treatment of elastoplastic systems. In: Nayroles B (Ed.) Applications of methods of functional analysis to problems in mechanics. Springer-Verlag, Berlin
36. **Moreau JJ** (1977) Evolution problem associated with a moving convex set in a Hilbert space. J. Differential Equations 26: 347–374
37. **Ogden RW** (1978) Nearly isochoric elastic deformations: Application to rubberlike solids. J. Mech. Phys. Solids 26: 37–57
38. **Ogden RW** (1997) Non-linear Elastic Deformations. Dover, New York
39. **Ogden RW, Roxburgh DG** (1999) An energy based model of the mullins effect. In: Dorfmann, A., Muhr, A. (Eds), Constitutive Models for Rubber, Rotterdam, A.A. Balkema. 23–28
40. **Oktay HS, Kang T, Humphrey JD, Bishop GG** (1991) Changes in the mechanical behavior of arteries following balloon angioplasty. In: ASME 1991 Biomechanics Symposium, AMD-Vol. 120 . American Society of Mechanical Engineers
41. **Ožbolt J, Bažant ZP** (1996) Numerical smeared fracture analysis: Nonlocal microcrack interaction approach. Int. J. Numer. Meth. Engr. 39: 635–661
42. **Parry DAD, Barnes GRG, Craig AS** (1978) A comparison of the size distribution of collagen fibrils in connective tissues as a function of age and a possible relation between fibril size distribution and mechanical properties. Proc. Roy. Soc. London Ser. B B203: 305–321
43. **Reese S** (2001) Meso-macro modelling of fiber-reinforced composites exhibiting elastoplastic material behavior. In: Proceedings of the 2nd European conference on computational mechanics, Cracow, Poland
44. **Ridge MD, Wright V** (1967) Mechanical properties of skin: A bioengineering study of skin structure. J. Appl. Physiol. 21: 1602–1606
45. **Salunke NV, Topoleski LDT** (1997) Biomechanics of atherosclerotic plaque. Crit. Rev. Biomed. Eng. 25: 243–285
46. **Schmidt-Baldassari M** (2001) Numerical concepts for rate-independent single crystal plasticity. submitted.
47. **Simo JC** (1987) A J_2-flow theory exhibiting a corner-like effect and suitable for large-scale computation. Comput. Meth. Appl. Mech. Engr. 62: 169–194
48. **Simo JC** (1998) Numerical analysis and simulation of plasticity. In: P. G. Ciarlet, J. L. Lions (Eds), Handbook of Numerical Analysis, Vol. VI, Amsterdam North-Holland, Elsevier. Numerical Methods for Solids (Part 3), 183-499
49. **Simo JC, Armero F, Taylor RL** (1993) Improved versions of assumed enhanced strain tri–linear elements for 3D finite deformation problems. Comput. Meth. Appl. Mech. Engr. 110: 359–386
50. **Simo JC, Hughes** (1998) Computational Inelasticity. New York: Springer-Verlag
51. **Simo JC, Kennedy JG, Govindjee S** (1988) Non-smooth multisurface plasticity and viscoplasticity Loading/unloading conditions and numerical algorithms. Int. J. Numer. Meth. Engr. 26: 2161–2185
52. **Simo JC, Oliver J, Amero F** (1993) An analysis of strong discontinuities induced by strain softening in rate-independent inelastic solids. Int. J. Numer. Meth. Engr. 2: 277–296
53. **Simo JC, Taylor RL, Pister KS** (1985) Variational and projection methods for the volume constraint in finite deformation elasto-plasticity. Comput. Meth. Appl. Mech. Engr. 51: 177–208
54. **Spencer AJM** (1984) Constitutive theory for strongly anisotropic solids. In: Spencer A J M (Ed) Continuum Theory of the Mechanics of Fibre-Reinforced Composites, pp. 1–32. Springer-Verlag, Wien, CISM Courses and Lectures No. 282, International Centre for Mechanical Sciences
55. **Sverdlik A, Lanir Y** (2002) Time-dependent mechanical behavior of sheep digital tendon, including the effects of preconditioning. J. Biomech. 124: 78–84
56. **Tanaka E, Yamada H** (1990) An inelastic constitutive model of blood vessels. Acta Mech. 82: 21–30
57. **Tanaka E, Yamada H, Murakami S** (1996) Inelastic constitutive modeling of arterial and ventricular walls. In: K. Hayashi, H. Ishikawa (Eds), Computational Biomechanics, Tokyo, Springer-Verlag. 137–163
58. **Taylor RL** (2000) FEAP – A Finite Element Analysis Program – Version 7.3. Berkeley: University of California
59. **Weiss JA, Maker BN, Govindjee S** (1996) Finite element implementation of incompressible, transversely isotropic hyperelasticity. Comput. Meth. Appl. Mech. Engr. 135: 107–128
60. **Wilkins ML** (1964) Calculation of elastic-plastic flow. In: Alder B, Fernbach S, Rotenberg M (eds), Methods in Computational Physics, Vol. 3, pp. 211–263. New York: Academic Press
61. **Zienkiewicz OC, Taylor RL** (2000) The Finite Element Method. Solid Mechanics, Vol 2. 5th edition Oxford: Butterworth Heinemann